UC Berkeley
UC Berkeley Electronic Theses and Dissertations

Title

Novel Regulators of Differentiation and Thermogenesis in Adipocytes

Permalink

https://escholarship.org/uc/item/2j96802c

Author

Tabuchi, Chihiro

Publication Date

2022

Peer reviewed|Thesis/dissertation

eScholarship.org Powered by the California Digital Library
University of California

Novel Regulators of Differentiation and Thermogenesis in Adipocytes

By

Chihiro Tabuchi

A dissertation submitted in partial satisfaction of the
requirements for the degree of
Doctor of Philosophy
in
Metabolic Biology
in the
Graduate Division
of the
University of California, Berkeley

Committee in charge:

Professor Hei Sook Sul, Chair
Professor Jen-Chywan Wang
Professor Kaoru Saijo

Fall 2022

Abstract

Novel Regulators of Brown Adipocyte Differentiation and Thermogenesis

By

Chihiro Tabuchi

Doctor of Philosophy in Metabolic Biology

University of California, Berkeley

Professor Hei Sook Sul

While white adipose tissue (WAT) stores excess energy as triglycerides, brown adipose tissue (BAT) dissipates heat through uncoupling protein 1 (UCP1) by utilizing fuels such as fatty acids and glucose. A third type of adipocytes are beige adipocytes, which arise in WAT depots upon certain stimuli and are capable of thermogenesis, whose process is called browning or beiging. Since the recent discovery of active BAT or BAT-like tissue in human adults, targeting BAT has been proposed as an attractive strategy to fight against obesity and its associated diseases as there are currently no effective treatments other than lifestyle changes. Regardless, the mechanisms underlying BAT differentiation and thermogenesis are not fully understood. The aim of my dissertation work was to identify and characterize novel regulators of BAT differentiation and thermogenesis.

Chapter 1 reviews the current knowledge on signaling pathways that regulate thermogenesis in adipocytes. Upon cold exposure, norepinephrine is released and activates β_3-adrenergic signaling in BAT. This causes activation of UCP1, upregulation of thermogenic genes, and increase in substrate supply for thermogenesis. Additionally, insulin/IGF-1 signaling is also important for BAT development as well as browning of WAT. The involvement of other signaling pathways such as those for thyroid hormone and TGFβ superfamily are also discussed.

Chapter 2 is to identify and characterize novel thermogenic genes in brown adipocytes. By utilizing CRISPR-Cas9 screening along with a temperature-sensitive dye, I identified Apold1, which is enriched in BAT and responsive to β_3-adrenergic stimuli. Through *in vitro* gain-of-function and loss-of-function experiments, I confirmed that Apold1 indeed promotes thermogenesis. Unexpectedly, Apold1 global knockout mice showed lower body weight due to reduced food intake. Thus, the tissue-specific role of Apold1 was examined by viral injection of Apold1 into BAT, which increased body temperature and oxygen consumption in mice.

Chapter 3 describes another screening effort to identify novel thermogenic regulators. Using a different dye as a readout for thermogenesis, I found Rasl12 to promote thermogenesis in brown adipocytes. The role of Rasl12 on thermogenesis was verified by *in vitro* experiments. Interestingly, co-immunoprecipitation combined with mass spectrometry revealed the possible

interaction of Rasl12 with nuclear transporters and RNA processing factors, which is an unexplored aspect of thermogenesis regulation.

Chapter 4 profiles yet another screening effort to identify and characterize novel regulators for brown adipocyte differentiation. I found Zc2hc1c, which suppressed brown adipocyte differentiation when overexpressed. RNA-sequencing and RT-qPCR revealed that Zc2hc1c KO cells had increased expression of PPARγ, a master regulator of adipocyte differentiation, suggesting the inhibitory effect of Zc2hc1c on differentiation.

Lastly, chapter 5 concludes my work describing the importance of novel genes identified in BAT thermogenesis and differentiation, future directions and remaining questions.

All together, these studies have identified novel regulators of thermogenesis and differentiation in brown adipocytes, which will provide a better understanding of BAT biology and advance the field to combat obesity.

Table of Contents

Abstract..…… 1
Table of Contents...…… i
List of Figures…….. iii
List of Tables…… iv
Acknowledgments..…… v

Chapter 1: Signaling Pathways Regulating Thermogenesis……..…… 1
Abstract…… 2
Introduction…….. 2
β_3-adrenergic signaling..…… 3
Insulin/IGF1 signaling…….. 5
Thyroid hormone…….. 6
Transforming growth factor β family…… 7
Concluding remark…… 9
References……. 9

Chapter 2: Apold1 is a novel activator of thermogenesis in brown adipocytes……..…….. 16
Abstract……... 17
Introduction…….…… 17
Results…….…… 18
Discussion…….…... 20
Experimental procedures…….…… 21
Acknowledgements…….…… 23
References…….…... 23

Chapter 3: Rasl12 promotes thermogenesis through nuclear transport……..…….. 32
Abstract……33
Introduction……..33
Results……..34
Discussion……35
Experimental procedures……..36
Acknowledgements……..38
References……38

Chapter 4: Zc2hc1c suppresses brown adipocyte differentiation….……46
Abstract…… 47
Introduction…….. 47
Results…….. 48

Discussion……49
Experimental procedures……. 49
Acknowledgements……..51
References……51

Chapter 5: Conclusion……..……. 56
References……58

List of Figures

Chapter 1

Figure 1. Schematic model of β_3-adrenergic signaling pathway that promotes thermogenesis in adipocytes. ……..……..14

Figure 2. Schematic models of BMP7 and TGF b signaling pathways in thermogenesis..…..…15

Chapter 2

Figure 1. CRISPR-Cas9 screening identified Apold1 as a potential thermogenic activator.…... 26

Figure 2. Characterization of Apold1 *in vitro*..……..…….. 27

Figure 3. Apold1 promotes thermogenesis *in vitro*. ……..……...28

Figure 4. Characterization of Apold1 global knockout mice and BAT-specific overexpression in mice.…..…….29

Chapter 3

Figure 1. Identification and characterization of Rasl12..……..……... 40

Figure 2. Rasl12 promotes thermogenesis *in vitro*……..…….....42

Figure 3. Rasl12 localization and potential interacting partners. ……..……...43

Chapter 4

Figure 1. Characterization of Zc2hc1c. ……...…….……52

Figure 2. Zc2hc1c inhibits brown adipocyte differentiation.. …….…….53

Figure 3. RNA-sequencing of Zc2hc1c KO cells……..…….……..54

List of Tables

Chapter 2
Table 1: List of primers for RT-qPCR. ……..…….30
Table 2: List of antibodies used. …….31

Chapter 3
Table 1: List of primers for RT-qPCR. ……..……..44
Table 2: List of antibodies used. …….45

Chapter 4
Table 1: List of primers for RT-qPCR. ……...55

Acknowledgements

First and foremost, I would like to express my deepest gratitude to my boss, advisor and mentor Dr. Hei Sook Sul for taking me into her lab and training me for 5 years. The mentorship you gave me and the amount of learning I had from her knowledge and experience were unimaginable and I am certain that these experiences will greatly help me advance my career in the future. Thank you to all of my qualifying exam committee and thesis committee members, Jen-Chywan Wang, Kaoru Saijo and James Olzmann, for their support and guidance over the years.

I would not have been able to accomplish nearly as much as I have without the help of my lab members. I would also like to thank my undergraduate students for their help in doing experiments.

Lastly, thanks to my friends and family who made it possible for me to pursue my career.

Chapter 1
Signaling Pathways Regulating Thermogenesis

Signaling pathways regulating thermogenesis

Abstract

Obesity, an excess accumulation of white adipose tissue (WAT), has become a global epidemic and is associated with complex diseases, such as type 2 diabetes and cardiovascular diseases. Presently, there are no safe and effective therapeutic agents to treat obesity. In contrast to white adipocytes that store energy as triglycerides in unilocular lipid droplet, brown and brown-like or beige adipocytes utilize fatty acids (FAs) and glucose at a high rate mainly by uncoupling protein 1 (UCP1) action to uncouple mitochondrial proton gradient from ATP synthesis, dissipating energy as heat. Recent studies on the presence of brown or brown-like adipocytes in adult humans have revealed their potential as therapeutic targets in combating obesity. Classically, the main signaling pathway known to activate thermogenesis in adipocytes is β_3-adrenergic signaling, which is activated by norepinephrine in response to cold, leading to activation of the thermogenic program and browning. In addition to the β_3-adrenergic signaling, numerous other hormones and secreted factors have been reported to affect thermogenesis. In this review, we discuss several major pathways, β_3-adrenergic, insulin/IGF1, thyroid hormone and TGFβ family, which regulate thermogenesis and browning of WAT.

Keywords: Thermogenesis, UCP1, brown adipose tissue, beige/brite adipocytes, browning/beiging, β_3-adrenergic signaling, insulin/IGF1 signaling, thyroid hormone, TGFβ superfamily

Introduction

Brown adipose tissue (BAT) is specialized in heat production through non-shivering thermogenesis by burning fuels such as fatty acids (FA) and glucose (Nedergaard and Cannon 2018). BAT is crucial for maintaining body temperature especially for infants who have limited ability to perform shivering thermogenesis, due to underdeveloped skeletal muscle (Lidell 2019). In adults, BAT contributes to energy expenditure as indicated by an inverse correlation between the presence of active BAT and central obesity (Q. Wang et al. 2015; Saito 2013). In addition to numerous mitochondria, BAT possesses multilocular lipid droplets that provide FAs for β-oxidation, which drives tricarboxylic acid (TCA) cycle and electron transport chain (ETC) to create proton gradient (Fenzl and Kiefer 2014). In contrast, white adipose tissue (WAT) serves as an energy storage and has a unilocular lipid droplet and fewer mitochondria.

Of all tissues, BAT expresses the highest levels of uncoupling protein 1 (UCP1) and UCP1 plays a central role in non-shivering thermogenesis (Lattin et al. 2008). UCP1 acts as a proton transporter in the inner membrane of mitochondria, which allows protons to leak from intermembrane space into the mitochondrial matrix (Chouchani, Kazak, and Spiegelman 2018). This uncouples the proton gradient from ATP synthesis, dissipating the proton gradient in the form of heat. Therefore, having a large number of mitochondria and multilocular lipid droplets enables BAT to maximize its thermogenic capacity. Although WAT normally has little UCP1 expression, some cells in subcutaneous WAT depots display thermogenic capacity with elevated UCP1 expression upon certain stimulations, the process so-called ‘browning/beiging’ (Herz and Kiefer 2019). These thermogenic adipocytes are termed ‘beige/brite’ adipocytes, which seem to originate from different precursor cells than brown adipocytes, based on distinct gene signatures (Wu et al. 2012). However, transdifferentiation of mature white adipocytes to thermogenic beige

adipocytes have also been reported (Shao et al. 2019). It is plausible that these thermogenic adipocytes can be generated by distinct mechanisms.

Classical brown adipocytes originate from a subset of multipotent stem cells in the dermomyotome that express engrailed 1 (EN1), paired box 7 (PAX7) and myogenic factor 5 (MYF5) (W. Wang and Seale 2016). While the $MYF5^{+}/PAX7^{+}/EN1^{+}$ progenitor cells can give rise to other cell types, such as skeletal myocytes, they commit to brown adipocyte lineage upon early B cell factor 2 (EBF2) expression (Rajakumari et al. 2013). Additionally, PR domain containing 16 (PRDM16) stimulates brown adipocyte differentiation over myoblast differentiation through the interaction with peroxisome proliferator activated receptor γ (PPARγ) (Seale et al. 2008). Ewing Sarcoma (EWS)/Y-box binding protein 1 (YBX1) complex promotes bone morphogenetic protein 7 (BMP7) transcription, which also determines brown adipocyte lineage during development (Park et al. 2013). Committed brown precursor cells then differentiate into mature brown adipocytes through a series of transcriptional events (Inagaki, Sakai, and Kajimura 2016; W. Wang and Seale 2016). ZFP516 stimulates thermogenic gene expression such as UCP1, DIO2 and CIDEA to promote brown adipocyte differentiation. ZFP516 interacts with not only PRDM16 , but also with LSD1 in activating thermogenic gene program. ZC3H10 upregulates transcription of genes for mitochondrial biogenesis, such as NRF1 and TFAM (Dempersmier et al. 2015; Yi et al. 2019). EBF2 activates transcription of PPARγ, which promotes expression of numerous lipid metabolic genes, such as fatty acid binding protein (FABP4/aP2), cluster of differentiation 36 (CD36) and lipoprotein lipase (LPL) (Koppen and Kalkhoven 2010). In addition, EBF2 and PPARγ cooperatively activate transcription of PRDM16. CEBPβ also activates PPARγ transcription to promote adipogenic and thermogenic gene expression (Kajimura et al. 2009). PPARγ coactivator α (PGC1α) is another transcriptional co-regulator that interacts with many proteins including PPARγ, PRDM16 and IRF4 to promote BAT development, especially mitochondrial biogenesis through NRF1 and TFAM (Gill and La Merrill 2017; Inagaki, Sakai, and Kajimura 2016). Some of the aforementioned transcription factors and co-activators such as ZFP516, ZC3H10 and PGC1α also induce thermogenic gene expression upon β_3-adrenergic stimuli in mature brown and white adipocytes, the latter of which leads to browning.

Environmental cues such as cold exposure, exercise and diet can trigger non-shivering thermogenesis in classical BAT and also browning of WAT, by activating specific signaling cascades within the cell (Ikeda, Maretich, and Kajimura 2018; Gill and La Merrill 2017). For example, cold temperature stimulates the sympathetic nervous system to release norepinephrine, which then binds β_3-adrenergic receptor (Inagaki, Sakai, and Kajimura 2016). β_3-adrenergic signaling has a wide range of downstream targets including numerous transcription factors and co-activators that can induce thermogenic genes (Yi, Nguyen, and Sul 2020). In addition to the transcriptional regulation, β_3-adrenergic signaling also increases lipolysis and glucose uptake to support thermogenesis (Reverte-Salisa, Sanyal, and Pfeifer 2019). In this review, we discuss underlying signaling pathways that regulate thermogenesis in brown and beige adipocytes, as well as browning of WAT.

1. β_3-Adrenergic signaling

The dominant signaling pathway that governs non-shivering thermogenesis in brown and beige adipocytes is β_3-adrenergic signaling. Upon cold exposure, norepinephrine released from the sympathetic nervous system binds mainly β_3-adrenergic receptor (β_3-AR) to induce adrenergic signaling (J. Liu, Wang, and Lin 2019; Schena and Caplan 2019). β_3-AR coupled with

Gs activates AC, which in turn produces cAMP for PKA activation. A variety of downstream targets of PKA, such as p38, CREB and HSL, enhances thermogenesis by inducing thermogenic gene expression and/or mobilizing substrate to fuel thermogenesis (Shi and Collins 2017; Cao et al. 2004).

p38, a MAP kinase, phosphorylates multiple transcription factors, including ATF2 and IRF4, both of which can bind to the enhancer or promoter regions to activate UCP1 transcription (Yi, Nguyen, and Sul 2020). In addition, we recently found that ZC3H10, previously known to bind RNA, is phosphorylated by p38 upon cold, activating the thermogenic gene program in adipocytes (Yi et al. 2019). Specifically, ZC3H10 binds a distal upstream region of the UCP1 promoter for transcriptional activation. ZC3H10 also activates NRF1 and TFAM, which facilitate mitochondrial biogenesis to increase thermogenic capacity of adipocytes. Thus, transgenic mice overexpressing ZC3H10 exhibited increased oxygen consumption, higher BAT temperature and reduced body weight while ZC3H10 knockout mice displayed decreased oxygen consumption, lower BAT temperature and increased body weight. PGC1α is also a downstream target of p38 and serves as co-activator for PPARγ and NRF1 to promote expression of UCP1 and TFAM, respectively (Cao et al. 2004; Liang and Ward 2006). Similarly, CREB activates various thermogenic genes, such as UCP1, PGC1α and DIO2 (S. Wang et al. 2019).

β_3-adrenergic signaling also increases the expression of ZFP516. ZFP516 recruits LSD1, which demethylases H3K9 at the proximal region of UCP1 promoter to induce UCP1 transcription. Furthermore, ZFP516 directly interacts with PRDM16 at the UCP1 promoter and potentially at other BAT gene promoters. ZFP516 depletion *in vivo* resulted in impaired BAT formation with decreased BAT gene expression and increased muscle gene expression in the presumptive BAT depot, while ZFP516 overexpression increased body temperature, oxygen consumption, browning of WAT, leading to lower body weight. Taken together, ZFP516 is required for BAT development in addition to promoting WAT browning.

Adipose thermogenesis can be enhanced by an increased supply of substrates such as FA and glucose. Upon β_3-AR activation, PKA phosphorylates HSL, now known as diacylglycerol hydrolase, as well as PLIN on lipid droplets to promote lipolysis. FAs thus produced upon lipolysis can undergo β-oxidation to eventual production of NADH and FADH for ETC, during UCP1-mediated thermogenesis (Fenzl and Kiefer 2014; Symonds 2017). FA also directly binds UCP1 to assist proton influx into the mitochondrial matrix (Kajimura and Saito 2014). In the fed state, however, FAs as substrates for thermogenesis seem to originate from white adipose tissue lipolysis, although it was also reported that inhibition of intracellular lipolysis suppressed cold-induced non-shivering thermogenesis in BAT, which was compensated by an increased shivering in humans (Blondin et al. 2017; Shin et al. 2017). Of note, lipolysis can also be modulated non-adrenergically and this aspect has been extensively reviewed elsewhere (Braun et al. 2018).

We recently discovered a BAT-specific NADH oxidase, AIFM2, which is required for cold- and diet-induced thermogenesis (Nguyen et al. 2020). Upon cold or β_3-adrenergic stimuli, AIFM2 translocates from lipid droplet to the outer side of the inner membrane of mitochondria. AIFM2 oxidizes NADH to NAD which is needed for glyceraldehyde-3 phosphate dehydrogenase (GAPDH) reaction, in supporting robust glycolysis. In addition, electrons generated from AIFM2 action are transferred to CoQ for ETC activity of mitochondria. AIFM2 KO mice exhibited higher body weight, lower oxygen consumption, and lower BAT temperature whereas AIFM2 overexpression resulted in the opposite phenotypes. In addition, the expression of AIFM2 was induced upon refeeding with high carb diet when examined at thermoneutrality,

suggesting that glucose oxidation appears to be especially important in the fed state to promote thermogenesis when the blood glucose level is relatively high.

Collectively, there is no doubt that β_3-AR signaling plays a dominant role in regulating thermogenesis. Besides those mentioned above, there are many more proteins that are involved in and downstream of β_3-AR signaling. Further studies will elucidate more components related to β_3-AR signaling that regulate thermogenesis at various steps such as substrate metabolism, mitochondrial homeostasis, gene expression as well as signal transduction.

2. Insulin/IGF1 signaling

Insulin/IGF1 signaling plays important roles in adipose tissue development and thermogenesis. Mice with fat-specific double knockout of insulin receptor (IR) and IGF1 receptor (IGF1R) (FIGIRKO) exhibited decreased adiposity with more than 85% reduction in BAT, having lower body weight (Boucher et al. 2012). Indeed, brown preadipocytes from FIGIRKO failed to differentiate *in vitro* with no increase in the expression of PPARγ and CEBPα, indicating that insulin/IGF-1 signaling is critical for BAT development. Since the addition of PPARγ agonist, rosiglitazone, did not rescue the impaired differentiation, insulin/IGF-1 signaling seemed to act on the upstream of PPARγ/CEBPα. Consistently, phosphorylation of CEBPβ at Thr188, which is required for DNA binding and therefore transcriptional activation of PPARγ/CEBPα, was reduced. FIGIRKO mice were also protected from diet-induced obesity, possibly due to impaired adipose development. FIGIRKO mice failed to maintain their body temperature during cold exposure, although they had higher energy expenditure/basal metabolic rate with no change in activity, this paradox remaining to be explained. In this regard, the study utilized aP2 promoter to express Cre recombinase for gene KO, which could have affected not only adipose tissues but also other cell types, such as macrophages.

The effects of insulin signaling and IGF-1 signaling were further investigated by comparing fat-specific IR single KO (F-IRKO) and IGF1R single KO (F-IGFRKO) to IR/IGF1R double KO (F-IR/IGFRKO), which were all generated by Cre driven by adiponectin promoter (Boucher et al. 2016). F-IGFRKO only had a small reduction in both WAT and BAT, while F-IR/IGFRKO had an almost complete loss of adipose tissue. Interestingly, F-IRKO had a large WAT reduction with an unexplainable 50% increase in BAT with large unilocular lipid droplet. BAT of F-IR/IGFRKO exhibited increased BAT gene expression and decreased WAT gene expression, whereas that of F-IRKO showed no change in BAT or WAT marker gene expression. Regardless, the expression of genes involved in BAT function, including UCP1 and other thermogenic genes, TFAM for example, was reduced in both F-IR/IGFRKO and F-IRKO, which could explain why both F-IR/IGFRKO and F-IRKO failed to maintain body temperature during the cold challenge. Indeed, F-IRKO had reduced mitochondrial content and oxygen consumption.

BAT-specific IR KO mice created by using UCP1 promoter-Cre, however, showed impaired BAT development (Guerra et al. 2001). Since the expression of CEBPα, but not PPARγ, decreased in BAT of the KO mice, insulin signaling likely promotes brown adipogenesis mainly through CEBPα. Interestingly, UCP1 expression increased significantly in BAT and the KO mice even had leaner phenotype, possibly due to the remaining BAT compensating for the decreased thermogenesis. Another mechanism where insulin/IGF1 signaling can promote BAT development is by increasing proliferation. Insulin and IGF1, not only stimulated IRS1 and IRS2 tyrosine phosphorylation and their association with PI3K, but also enhanced IRS1-associated

GRB2 phosphorylation, which can activate RAS-MAPK pathway for proliferation (Valverde et al. 1998). BAT-specific IGF1R KO mice, on the other hand, had normal BAT size and normal body weight, while UCP1 expression in BAT was reduced and the KO mice were cold intolerant, suggesting that IGF1 signaling enhances BAT thermogenesis (Viana-Huete et al. 2016).

Insulin/IGF1 signaling plays a role in browning of WAT as well. PTEN antagonizes the action of PI3K by converting PIP3 back to PIP2 and, therefore, insulin/IGF1 signaling. PTEN knockdown (KD) by direct injection of Rec2-Cre in iWAT of PTEN floxed mice increased AKT signaling and induced browning (Huang et al. 2019). These effects were blocked by administration of an AKT inhibitor, indicating that the PI3K-AKT pathway promotes browning. Transgenic mice overexpressing PTEN were reported to have increased energy expenditure with hyperactivation of BAT. However, PTEN was overexpressed globally in these animals, making it difficult to interpret the exact contribution of PTEN in a tissue-specific manner (Ortega-Molina et al. 2012).

Interestingly, insulin signaling can be modulated by β_3-adrenergic signaling. β_3-adrenergic signaling pretreatment reduced the activation of IR, IRS1 and IRS2. In addition, β_3-adrenergic signaling mitigated AKT activation and IRS1-associated activation of PI3K upon insulin treatment, while it did not affect MAPK activation and IRS2-associated activation of PI3K. Moreover, β_3-adrenergic signaling abolished insulin-mediated glucose uptake in brown adipocytes (Klein et al. 1999). In this regard, cold exposure has also been shown to alter the expression of many molecules involved in the insulin signaling pathway (X. Wang and Wahl 2014). Specifically, the expression of IRS1 and IRS2 as well as phosphorylation of AKT are upregulated. These discrepancies could be due to the differences in the methods used such as *in vitro* vs *in vivo*, mouse vs rat as well as protein phosphorylation vs transcriptome.

Taken together, IR/IGF1R signaling promotes adipose tissue thermogenesis by supporting BAT development, browning of WAT and BAT function. Some of those studies mentioned above are even conflicting, owing at least partly to the differences in promoters used to express Cre, which affects not only the efficiency of gene KO, but also tissue specificity. Even with a tissue-specific KO, some phenotypes could manifest because of secondary effects rather than direct, primary effects. Therefore, it would be important to recapitulate the results *in vitro* as well. Further research is needed to better clarify the role of IR and IGF1R signaling in adipose tissue thermogenesis.

3. Thyroid hormone

Among various ligands/hormones that bind and function via nuclear hormone receptors, thyroid hormone (TH) is classically known to regulate thermogenesis (Yau and Yen 2020). TH receptors (TR), TRα and TRβ, in adipocytes enhance BAT thermogenesis and WAT browning. TRs are activated by triiodothyronine (T3), an active form of TH produced from thyroxine (T4) by type II iodothyronine deiodinase (DIO2). Although TRα and TRβ may have overlapping functions, TRβ seems mainly responsible for UCP1 induction, whereas TRα might be more important for full β_3-adrenergic response. In hypothyroid mice, TRβ-selective ligand, GC-1, restored UCP1 expression to the same extent as T3, suggesting the significant role of TRβ in UCP1 upregulation (M. O. Ribeiro et al. 2001). However, GC-1-treated mice failed to maintain body temperature during cold exposure, suggesting that UCP1 induction by TRβ alone is not sufficient to support thermogenesis. In agreement with this, GC-1 treatment did not restore cAMP production in isolated brown adipocytes of the hypothyroid mice, which suggests the involvement of TRα in β_3-adrenergic response. The same group later showed that hypothyroid

mice with a dominant negative TRβ mutation failed to increase UCP1 expression in BAT (Miriam O. Ribeiro et al. 2010). These hypothyroid TRβ mutant mice also had reduced cAMP production in BAT and lower body temperature upon T3 replacement and β_3-adrenergic stimulation, implying that TRβ might at least partly participate in β_3-adrenergic response. Although it has also been reported that TRα could bind UCP1 enhancer region for transcriptional activation, the results of the study were relied on *in vitro* experiments as opposed to the previously mentioned studies that investigated its role in animal models (Chen, Yang, and Roeder 2009). DIO2 is another important TH/TR target that contributes to thermogenesis. GC-1 upregulated DIO2 mRNA and enzyme activity upon β_3-adrenergic stimulation, while TRα-selective ligand, CO23, increased DIO2 mRNA expression only (Martinez de Mena, Scanlan, and Obregon 2010). Indeed, DIO2 KO brown adipocytes exhibited reduced UCP1 expression, oxygen consumption and lipolysis in response to β3-adrenergic stimuli, which was reversed by T3 administration (de Jesus et al. 2001).

TH/TR can enhance BAT thermogenesis through regulation of mitochondrial homeostasis as well (Yau et al. 2019). Hyperthyroid mice showed increased expression of mitochondrial proteins including COX4I1 and TOMM20 and increased mitochondrial DNA copy number in BAT, implying that TH promoted mitochondrial biogenesis. On the other hand, T3-treated brown adipocytes exhibited mitochondrial remnants inside autophagic vesicles, suggesting that T3 induced mitophagy. Inhibition of autophagy/mitophagy in hyperthyroid mice indeed increased mitochondrial proteins. Mitochondrial turnover was further assessed using MitoTimer, which showed upregulation of both clearance of mature mitochondria and generation of new mitochondria by T3 treatment. The importance of mitochondrial turnover for thermogenesis was confirmed by suppression of autophagy/mitophagy by ATG5 KD, which decreased oxygen consumption in brown adipocytes, and also conditional ATG5 KO in hyperthyroid mice that showed reduced body temperature.

T3 treatment has been shown to upregulate UCP1 and mitochondria-related genes in white adipocytes as well, by increasing mitochondrial biogenesis (J.-Y. Lee et al. 2012; Krause 2020). This was accompanied by elevated oxygen consumption and FA oxidation, indicating the role of T3 in WAT browning. Similar to that observed in brown adipocytes, UCP1 upregulation in WAT was mediated by TRβ rather than TRα since hyperthyroid TRβ KO mice failed to increase UCP1 expression in WAT (Johann et al. 2019). In addition to directly upregulating UCP1 transcription, T3 was reported also to trigger AMPK activation, which in turn activated the p38/ATF2 pathway to promote UCP1 expression in WAT, although the mechanism by which T3 could activate AMPK remains to be addressed (Matesanz et al. 2017).

Recently, a TH metabolite, 3,5 Diiodo-L-Thyronine (T2), was reported to affect thermogenesis as well (Louzada and Carvalho 2018). T2 administration restored lipid morphology, vascularization, innervation and mitochondrial content/activity in BAT of hypothyroid rats, which were accompanied by increased expression of UCP1 and PGC1α, leading to improved thermogenesis (Lombardi et al. 2015). Similarly, T2 seems to promote WAT browning in high fat diet-induced obese rats partly through upregulation of PRDM16 (Senese et al. 2019). Overall, it can be concluded that the TH/TR promotes BAT thermogenesis and WAT browning.

4. Transforming growth factor β superfamily

Multiple members of the transforming growth factor beta (TGFβ) superfamily have been shown to regulate thermogenesis. In fact, bone morphogenetic protein 7 (BMP7), was reported

first to trigger commitment of mesenchymal progenitor cells to brown adipocyte lineage by activating SMAD1/5/8 (Tseng et al. 2008). Without the canonical differentiation induction cocktail, BMP7 induced the expression of both adipogenic and brown-adipocyte specific genes, such as CEBPs, PPARγ, PRDM16, PGC1α, and UCP1, while downregulating adipogenic suppressors such as Pref-1 and WNT10A. BMP7 KO mice exhibited reduced BAT mass that had almost undetectable UCP1 expression. In contrast, BMP7 overexpression via adenovirus injection increased the expression of PRDM16 and UCP1 in BAT, energy expenditure and body temperature, while decreasing body weight. In mature brown adipocytes, BMP7 increased mitochondrial activity through p38-ATF2 and SMAD1/5/8 pathways (Townsend et al. 2013). BMP7-treated cells upregulated the expression of CD36 and CPT1 that transport FAs into the cells and mitochondria, respectively, resulting in increased citrate synthase activity and FA oxidation. Administration of BMP7 *in vivo* increased the expression of CD36 in BAT, which was accompanied by increased oxygen consumption. In addition, respiratory exchange ratio in these animals decreased, reflecting the substrate utilization switching towards fatty acids. Another study also confirmed the similar effects of BMP7, where BMP7 administration increased the expression of UCP1 and CD36 in BAT, BAT mass, energy expenditure and fat oxidation (Boon et al. 2013). Furthermore, these authors found that BMP7 induced the expression of BAT genes in WAT depots with overall reduced WAT size, suggesting that BMP7 promotes browning of WAT. This is supported by a finding that demonstrated BMP7 driving human adipogenic stem cells into beige adipocytes (Okla et al. 2015). BMP7 treatment promoted the expression of beige markers, such as CD137 and TMEM26, in addition to the expression of thermogenic genes, such as UCP1, CIDEA and DIO2.

BMP8b was found to be highly expressed in BAT and its expression increased during differentiation and during cold exposure (Whittle et al. 2012). BMP8b KO mice exhibited lower energy expenditure, lower body temperature and higher body weight, which were exacerbated when these mice were on high fat diet (HFD). Although BMP8b KO mice showed normal BAT size and BAT gene expression, activation of thermogenic signaling pathways examined by phosphorylation of SMAD1/5/8/, p38 and CREB were impaired, indicating that BMP8b is indispensable for thermogenic activation of BAT, but not for BAT development. Consistently, BMP8b treatment increased phosphorylation of these proteins in differentiated brown adipocytes, as well as that of HSL and AMPK, resulting in increased lipolysis measured by glycerol release. In addition, BMP8b promoted the activation of AMPK in the central nervous system as well, increasing sympathetic output to BAT to support thermogenesis. In this regard, BMP8b was shown to stimulate sympathetic innervation and vascularization through NRG4 and VEGF, respectively, in both BAT and WAT as well as browning of WAT (Pellegrinelli et al. 2018). Mice overexpressing BMP8b showed higher energy expenditure, lower body weight and fat mass, accompanied by decreased thermogenic gene expression in WAT that exhibited multilocular lipid droplets, whereas loss of BMP8b resulted in decreased nerve density.

TGFβ/SMAD3 signaling pathway has been reported to suppress browning of WAT (Yadav et al. 2011). TGFβ treatment suppressed activation of PGC1α promoter-reporter in

3T3-L1 cells, which was abolished by SMAD3 KD, indicating that TGFβ represses PGC1α transcription through SMAD3. SMAD3 KO animals had higher body temperature, lower body weight, lower blood glucose, and better response to insulin. WAT of SMAD3 KO mice indeed expressed thermogenic genes, such as UCP1, and exhibited multilocular morphology. Similarly, adipose-specific TGFβ receptor 1 (TGFβR1) KO induced browning, as evidenced by increased UCP1 expression in WAT on HFD, which was accompanied by lower body weight (Wankhade et al. 2018). TGFβR1 inhibitor, SB431542, induced brown and beige genes during differentiation of WAT SVF cells, whereas TβR1 downregulated those genes. Interestingly, WAT of TGFβR1 KO also increased the expression of genes involved in prostaglandin pathways, such as COX2, implying that prostaglandin pathway might be involved in browning of WAT. SMAD3 KD in 3T3-L1 cells increased the expression of COX2 and other prostaglandin pathway-related proteins. Treatment with PGE_2, a product of COX2, upregulated thermogenic gene expression, such as CIDEA1 and PGC1α, in the presumptive beige precursor cells, which was further augmented by the addition of SB431542, implying the possible interaction between TGFβ/SMAD3 and COX2/PGE_2 pathways. These presumptive beige precursor cells were isolated and selected from WAT by FACS using a series of cell surface markers and were termed inducible beige stem/progenitor cells (iBSCs). iBSCs were then transplanted subcutaneously into immunodeficient nude mice on HFD with IPTT-300 transponder. During the cold exposure, iBSCs from TβR1 KO mice maintained higher temperature and showed higher expression of thermogenic genes with multilocular lipid droplet morphology, suggesting that the KO iBSCs underwent beige adipogenesis. Altogether, TGFβ/SMAD3 signaling negatively regulates WAT browning although further research will help to clarify the contributions of different downstream pathways.

Concluding remark

The discovery of brown or brown-like adipocytes in human adults has made targeting adipocytes an attractive strategy to fight against obesity and its associated diseases. Activation of existing thermogenic adipocytes and/or induction of new thermogenic adipocytes can be mediated by various hormones and their signaling cascades, including those important pathways we describe in this review. Understanding the precise molecular mechanisms underlying regulation of thermogenesis and browning of WAT is critical for advancement of the future anti-obesity therapeutics.

References

Boon, Mariëtte R., Sjoerd A. A. van den Berg, Yanan Wang, Jan van den Bossche, Sofia Karkampouna, Matthias Bauwens, Marijke De Saint-Hubert, et al. 2013. “BMP7 Activates Brown Adipose Tissue and Reduces Diet-Induced Obesity Only at Subthermoneutrality.” *PloS One* 8 (9): e74083.

Boucher, Jeremie, Marcelo A. Mori, Kevin Y. Lee, Graham Smyth, Chong Wee Liew, Yazmin Macotela, Michael Rourk, Matthias Bluher, Steven J. Russell, and C. Ronald Kahn. 2012. “Impaired Thermogenesis and Adipose Tissue Development in Mice with Fat-Specific Disruption of Insulin and IGF-1 Signalling.” *Nature Communications* 3 (June): 902.

Boucher, Jeremie, Samir Softic, Abdelfattah El Ouaamari, Megan T. Krumpoch, Andre Kleinridders, Rohit N. Kulkarni, Brian T. O'Neill, and C. Ronald Kahn. 2016. "Differential Roles of Insulin and IGF-1 Receptors in Adipose Tissue Development and Function." *Diabetes* 65 (8): 2201–13.

Cao, Wenhong, Kiefer W. Daniel, Jacques Robidoux, Pere Puigserver, Alexander V. Medvedev, Xu Bai, Lisa M. Floering, Bruce M. Spiegelman, and Sheila Collins. 2004. "p38 Mitogen-Activated Protein Kinase Is the Central Regulator of Cyclic AMP-Dependent Transcription of the Brown Fat Uncoupling Protein 1 Gene." *Molecular and Cellular Biology* 24 (7): 3057–67.

Chouchani, Edward T., Lawrence Kazak, and Bruce M. Spiegelman. 2018. "New Advances in Adaptive Thermogenesis: UCP1 and Beyond." *Cell Metabolism*, November. https://doi.org/10.1016/j.cmet.2018.11.002.

Dempersmier, Jon, Audrey Sambeat, Olga Gulyaeva, Sarah M. Paul, Carolyn S. S. Hudak, Helena F. Raposo, Hiu-Yee Kwan, Chulho Kang, Roger H. F. Wong, and Hei Sook Sul. 2015. "Cold-Inducible Zfp516 Activates UCP1 Transcription to Promote Browning of White Fat and Development of Brown Fat." *Molecular Cell* 57 (2): 235–46.

Fenzl, A., and F. W. Kiefer. 2014. "Brown Adipose Tissue and Thermogenesis." *Hormone Molecular Biology and Clinical Investigation* 19 (1): 1868–91.

Gill, J. A., and Michele A. La Merrill. 2017. "An Emerging Role for Epigenetic Regulation of Pgc-1α Expression in Environmentally Stimulated Brown Adipose Thermogenesis." *Environmental Epigenetics* 3 (2): dvx009.

Guerra, C., P. Navarro, A. M. Valverde, M. Arribas, J. Brüning, L. P. Kozak, C. R. Kahn, and M. Benito. 2001. "Brown Adipose Tissue-Specific Insulin Receptor Knockout Shows Diabetic Phenotype without Insulin Resistance." *The Journal of Clinical Investigation* 108 (8): 1205–13.

Herz, Carsten T., and Florian W. Kiefer. 2019. "Adipose Tissue Browning in Mice and Humans." *The Journal of Endocrinology* 241 (3): R97–109.

Huang, Wei, Nicholas J. Queen, Travis B. McMurphy, Seemaab Ali, and Lei Cao. 2019. "Adipose PTEN Regulates Adult Adipose Tissue Homeostasis and Redistribution via a PTEN-Leptin-Sympathetic Loop." *Molecular Metabolism* 30 (December): 48–60.

Ikeda, Kenji, Pema Maretich, and Shingo Kajimura. 2018. "The Common and Distinct Features of Brown and Beige Adipocytes." *Trends in Endocrinology and Metabolism: TEM* 29 (3): 191–200.

Inagaki, Takeshi, Juro Sakai, and Shingo Kajimura. 2016. "Transcriptional and Epigenetic Control of Brown and Beige Adipose Cell Fate and Function." *Nature Reviews. Molecular Cell Biology* 17 (8): 480–95.

Johann, Kornelia, Anna Lena Cremer, Alexander W. Fischer, Markus Heine, Eva Rial Pensado, Julia Resch, Sebastian Nock, et al. 2019. "Thyroid-Hormone-Induced Browning of White Adipose Tissue Does Not Contribute to Thermogenesis and Glucose Consumption." *Cell Reports* 27 (11): 3385–3400.e3.

Kajimura, Shingo, and Masayuki Saito. 2014. "A New Era in Brown Adipose Tissue Biology: Molecular Control of Brown Fat Development and Energy Homeostasis." *Annual Review of Physiology* 76: 225–49.

Kajimura, Shingo, Patrick Seale, Kazuishi Kubota, Elaine Lunsford, John V. Frangioni, Steven P. Gygi, and Bruce M. Spiegelman. 2009. "Initiation of Myoblast to Brown Fat Switch by a PRDM16-C/EBP-Beta Transcriptional Complex." *Nature* 460 (7259): 1154–58.

Klein, Johannes, Mathias Fasshauer, Moriko Ito, Bradford B. Lowell, Manuel Benito, and C. Ronald Kahn. 1999. “β3-Adrenergic Stimulation Differentially Inhibits Insulin Signaling and Decreases Insulin-Induced Glucose Uptake in Brown Adipocytes.” *The Journal of Biological Chemistry* 274 (49): 34795–802.

Koppen, Arjen, and Eric Kalkhoven. 2010. “Brown vs White Adipocytes: The PPARgamma Coregulator Story.” *FEBS Letters* 584 (15): 3250–59.

Krause, Kerstin. 2020. “Novel Aspects of White Adipose Tissue Browning by Thyroid Hormones.” *Experimental and Clinical Endocrinology & Diabetes: Official Journal, German Society of Endocrinology [and] German Diabetes Association* 128 (6-07): 446–49.

Lattin, Jane E., Kate Schroder, Andrew I. Su, John R. Walker, Jie Zhang, Tim Wiltshire, Kaoru Saijo, et al. 2008. “Expression Analysis of G Protein-Coupled Receptors in Mouse Macrophages.” *Immunome Research* 4 (April): 5.

Lee, Joo-Young, Nobuyuki Takahashi, Midori Yasubuchi, Young-Il Kim, Hikari Hashizaki, Min-Ji Kim, Tomoya Sakamoto, Tsuyoshi Goto, and Teruo Kawada. 2012. “Triiodothyronine Induces UCP-1 Expression and Mitochondrial Biogenesis in Human Adipocytes.” *American Journal of Physiology. Cell Physiology* 302 (2): C463–72.

Liang, Huiyun, and Walter F. Ward. 2006. “PGC-1alpha: A Key Regulator of Energy Metabolism.” *Advances in Physiology Education* 30 (4): 145–51.

Lidell, Martin E. 2019. “Brown Adipose Tissue in Human Infants.” In *Brown Adipose Tissue*, edited by Alexander Pfeifer, Martin Klingenspor, and Stephan Herzig, 107–23. Cham: Springer International Publishing.

Liu, Jingxin, Yitao Wang, and Ligen Lin. 2019. “Small Molecules for Fat Combustion: Targeting Obesity.” *Acta Pharmaceutica Sinica. B* 9 (2): 220–36.

Lombardi, Assunta, Rosalba Senese, Rita De Matteis, Rosa Anna Busiello, Federica Cioffi, Fernando Goglia, and Antonia Lanni. 2015. “3,5-Diiodo-L-Thyronine Activates Brown Adipose Tissue Thermogenesis in Hypothyroid Rats.” *PloS One* 10 (2): e0116498.

Louzada, Ruy A., and Denise P. Carvalho. 2018. “Similarities and Differences in the Peripheral Actions of Thyroid Hormones and Their Metabolites.” *Frontiers in Endocrinology* 9 (July): 394.

Martinez de Mena, Raquel, Thomas S. Scanlan, and Maria-Jesus Obregon. 2010. “The T3 Receptor beta1 Isoform Regulates UCP1 and D2 Deiodinase in Rat Brown Adipocytes.” *Endocrinology* 151 (10): 5074–83.

Matesanz, Nuria, Edgar Bernardo, Rebeca Acín-Pérez, Elisa Manieri, Sonia Pérez-Sieira, Lourdes Hernández-Cosido, Valle Montalvo-Romeral, et al. 2017. “MKK6 Controls T3-Mediated Browning of White Adipose Tissue.” *Nature Communications* 8 (1): 856.

Nedergaard, Jan, and Barbara Cannon. 2018. “Brown Adipose Tissue as a Heat-Producing Thermoeffector.” *Handbook of Clinical Neurology* 156: 137–52.

Okla, Meshail, Jung-Heun Ha, Ryan E. Temel, and Soonkyu Chung. 2015. “BMP7 Drives Human Adipogenic Stem Cells into Metabolically Active Beige Adipocytes.” *Lipids* 50 (2): 111–20.

Ortega-Molina, Ana, Alejo Efeyan, Elena Lopez-Guadamillas, Maribel Muñoz-Martin, Gonzalo Gómez-López, Marta Cañamero, Francisca Mulero, et al. 2012. “Pten Positively Regulates Brown Adipose Function, Energy Expenditure, and Longevity.” *Cell Metabolism* 15 (3): 382–94.

Park, Jun Hong, Hong Jun Kang, Soo Im Kang, Ji Eun Lee, Jamie Hur, Kai Ge, Elisabetta Mueller, Hongjie Li, Byeong-Chel Lee, and Sean Bong Lee. 2013. “A Multifunctional

Protein, EWS, Is Essential for Early Brown Fat Lineage Determination." *Developmental Cell* 26 (4): 393–404.
Pellegrinelli, Vanessa, Vivian J. Peirce, Laura Howard, Samuel Virtue, Dénes Türei, Martina Senzacqua, Andrea Frontini, et al. 2018. "Adipocyte-Secreted BMP8b Mediates Adrenergic-Induced Remodeling of the Neuro-Vascular Network in Adipose Tissue." *Nature Communications* 9 (1): 4974.
Rajakumari, Sona, Jun Wu, Jeff Ishibashi, Hee-Woong Lim, An-Hoa Giang, Kyoung-Jae Won, Randall R. Reed, and Patrick Seale. 2013. "EBF2 Determines and Maintains Brown Adipocyte Identity." *Cell Metabolism* 17 (4): 562–74.
Reverte-Salisa, Laia, Abhishek Sanyal, and Alexander Pfeifer. 2019. "Brown Adipose Tissue: Role of cAMP and cGMP Signaling in Brown Fat." In *Brown Adipose Tissue*, edited by Alexander Pfeifer, Martin Klingenspor, and Stephan Herzig, 161–82. Cham: Springer International Publishing.
Ribeiro, Miriam O., Suzy D. C. Bianco, Masahiro Kaneshige, James J. Schultz, Sheue-Yann Cheng, Antonio C. Bianco, and Gregory A. Brent. 2010. "Expression of Uncoupling Protein 1 in Mouse Brown Adipose Tissue Is Thyroid Hormone Receptor-Beta Isoform Specific and Required for Adaptive Thermogenesis." *Endocrinology* 151 (1): 432–40.
Ribeiro, M. O., S. D. Carvalho, J. J. Schultz, G. Chiellini, T. S. Scanlan, A. C. Bianco, and G. A. Brent. 2001. "Thyroid Hormone--Sympathetic Interaction and Adaptive Thermogenesis Are Thyroid Hormone Receptor Isoform--Specific." *The Journal of Clinical Investigation* 108 (1): 97–105.
Saito, Masayuki. 2013. "Brown Adipose Tissue as a Regulator of Energy Expenditure and Body Fat in Humans." *Diabetes & Metabolism Journal* 37 (1): 22–29.
Schena, Giorgia, and Michael J. Caplan. 2019. "Everything You Always Wanted to Know about β3-AR * (* But Were Afraid to Ask)." *Cells* 8 (4). https://doi.org/10.3390/cells8040357.
Seale, Patrick, Bryan Bjork, Wenli Yang, Shingo Kajimura, Sherry Chin, Shihuan Kuang, Anthony Scimè, et al. 2008. "PRDM16 Controls a Brown Fat/skeletal Muscle Switch." *Nature* 454 (7207): 961–67.
Senese, Rosalba, Federica Cioffi, Rita De Matteis, Giuseppe Petito, Pieter de Lange, Elena Silvestri, Assunta Lombardi, Maria Moreno, Fernando Goglia, and Antonia Lanni. 2019. "3,5 Diiodo-L-Thyronine (T_2) Promotes the Browning of White Adipose Tissue in High-Fat Diet-Induced Overweight Male Rats Housed at Thermoneutrality." *Cells* 8 (3). https://doi.org/10.3390/cells8030256.
Shao, Mengle, Qiong A. Wang, Anying Song, Lavanya Vishvanath, Napoleon C. Busbuso, Philipp E. Scherer, and Rana K. Gupta. 2019. "Cellular Origins of Beige Fat Cells Revisited." *Diabetes* 68 (10): 1874–85.
Symonds, Michael E., ed. 2017. *Adipose Tissue Biology*. Springer, Cham.
Townsend, Kristy L., Ding An, Matthew D. Lynes, Tian Lian Huang, Hongbin Zhang, Laurie J. Goodyear, and Yu-Hua Tseng. 2013. "Increased Mitochondrial Activity in BMP7-Treated Brown Adipocytes, due to Increased CPT1- and CD36-Mediated Fatty Acid Uptake." *Antioxidants & Redox Signaling* 19 (3): 243–57.
Tseng, Yu-Hua, Efi Kokkotou, Tim J. Schulz, Tian Lian Huang, Jonathon N. Winnay, Cullen M. Taniguchi, T. Thien Tran, et al. 2008. "New Role of Bone Morphogenetic Protein 7 in Brown Adipogenesis and Energy Expenditure." *Nature* 454 (7207): 1000–1004.
Valverde, A. M., M. Lorenzo, S. Pons, M. F. White, and M. Benito. 1998. "Insulin Receptor Substrate (IRS) Proteins IRS-1 and IRS-2 Differential Signaling in the Insulin/insulin-like

Growth Factor-I Pathways in Fetal Brown Adipocytes." *Molecular Endocrinology* 12 (5): 688–97.
Viana-Huete, Vanesa, Carlos Guillén, Ana García-Aguilar, Gema García, Silvia Fernández, C. R. Kahn, and Manuel Benito. 2016. "Essential Role of IGFIR in the Onset of Male Brown Fat Thermogenic Function: Regulation of Glucose Homeostasis by Differential Organ-Specific Insulin Sensitivity." *Endocrinology* 157 (4): 1495–1511.
Wang, Qidi, Min Zhang, Min Xu, Weiqiong Gu, Yun Xi, Lu Qi, Biao Li, and Weiqing Wang. 2015. "Brown Adipose Tissue Activation Is Inversely Related to Central Obesity and Metabolic Parameters in Adult Human." *PloS One* 10 (4): e0123795.
Wang, Siyu, Min-Hsiung Pan, Wei-Lun Hung, Yen-Chen Tung, and Chi-Tang Ho. 2019. "From White to Beige Adipocytes: Therapeutic Potential of Dietary Molecules against Obesity and Their Molecular Mechanisms." *Food & Function* 10 (3): 1263–79.
Wang, Wenshan, and Patrick Seale. 2016. "Control of Brown and Beige Fat Development." *Nature Reviews. Molecular Cell Biology* 17 (11): 691–702.
Wang, Xiaofei, and Richard Wahl. 2014. "Responses of the Insulin Signaling Pathways in the Brown Adipose Tissue of Rats Following Cold Exposure." *PloS One* 9 (6): e99772.
Wankhade, Umesh D., Ji-Hyeon Lee, Pradeep K. Dagur, Hariom Yadav, Michael Shen, Weiping Chen, Ashok B. Kulkarni, et al. 2018. "TGF-β Receptor 1 Regulates Progenitors That Promote Browning of White Fat." *Molecular Metabolism* 16 (October): 160–71.
Whittle, Andrew J., Stefania Carobbio, Luís Martins, Marc Slawik, Elayne Hondares, María Jesús Vázquez, Donald Morgan, et al. 2012. "BMP8B Increases Brown Adipose Tissue Thermogenesis through Both Central and Peripheral Actions." *Cell* 149 (4): 871–85.
Wu, Jun, Pontus Boström, Lauren M. Sparks, Li Ye, Jang Hyun Choi, An-Hoa Giang, Melin Khandekar, et al. 2012. "Beige Adipocytes Are a Distinct Type of Thermogenic Fat Cell in Mouse and Human." *Cell* 150 (2): 366–76.
Yadav, Hariom, Celia Quijano, Anil K. Kamaraju, Oksana Gavrilova, Rana Malek, Weiping Chen, Patricia Zerfas, et al. 2011. "Protection from Obesity and Diabetes by Blockade of TGF-β/Smad3 Signaling." *Cell Metabolism* 14 (1): 67–79.
Yau, Winifred W., Brijesh K. Singh, Ronny Lesmana, Jin Zhou, Rohit A. Sinha, Kiraely A. Wong, Yajun Wu, et al. 2019. "Thyroid Hormone (T3) Stimulates Brown Adipose Tissue Activation via Mitochondrial Biogenesis and MTOR-Mediated Mitophagy." *Autophagy* 15 (1): 131–50.
Yau, Winifred W., and Paul M. Yen. 2020. "Thermogenesis in Adipose Tissue Activated by Thyroid Hormone." *International Journal of Molecular Sciences* 21 (8). https://doi.org/10.3390/ijms21083020.
Yi, Danielle, Jon M. Dempersmier, Hai P. Nguyen, Jose A. Viscarra, Jennie Dinh, Chihiro Tabuchi, Yuhui Wang, and Hei Sook Sul. 2019. "Zc3h10 Acts as a Transcription Factor and Is Phosphorylated to Activate the Thermogenic Program." *Cell Reports* 29 (9): 2621–33.e4.
Yi, Danielle, Hai P. Nguyen, and Hei Sook Sul. 2020. "Epigenetic Dynamics of the Thermogenic Gene Program of Adipocytes." *Biochemical Journal* 477 (6): 1137–48.

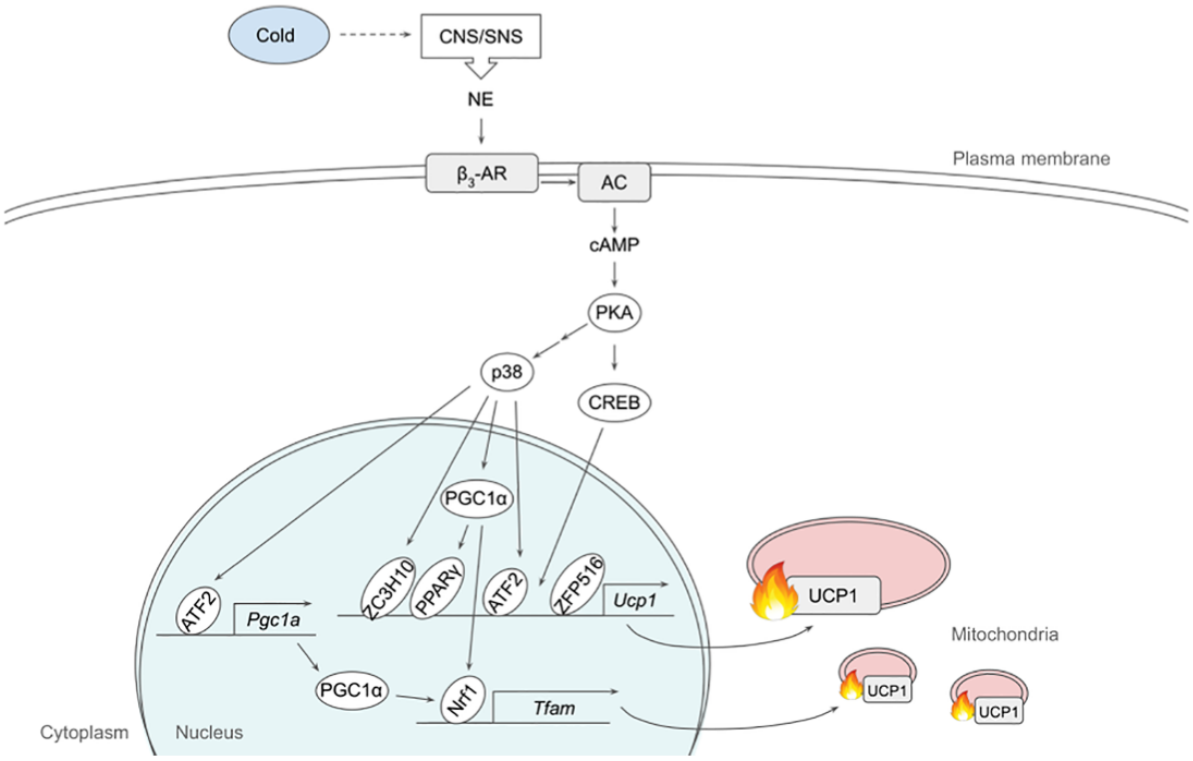


Figure 1. Schematic model of β_3-adrenergic signaling pathway that promotes thermogenesis in adipocytes. Cold stimulates CNS/SNS to secrete NE that binds β_3-AR, which then activates AC producing cAMP. cAMP in turn activates PKA that has a variety of downstream targets, including transcription factors to upregulate thermogenic gene expression. See text for details. AC, adenylate cyclase; ATF2, activating transcription factor 2; β_3-AR, β_3-adrenergic receptor; CNS, central nervous system; CREB, cAMP response-element binding protein; ETC, electron transport chain; FFA, free fatty acid; IRF4, interferon regulatory factor 4; NE, norepinephrine; NRF1, nuclear respiratory factor 1; PGC1α, peroxisome proliferator activated receptor γ coactivator α; PKA, protein kinase A; PPARγ, peroxisome proliferator activated receptor γ; SNS sympathetic nervous system; TCA, tricarboxylic acid; TFAM, mitochondrial transcription factor A; UCP1, uncoupling protein 1; ZC3H10, zinc finger CCCH-type containing 10; ZFP516, zinc finger protein 516.

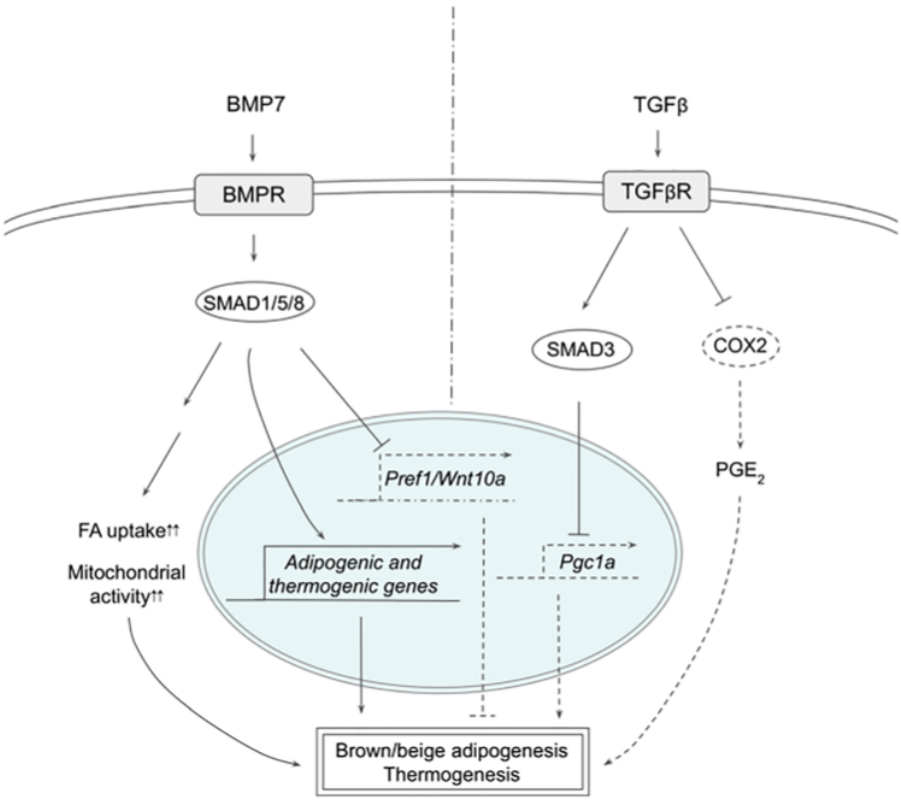


Figure 2. Schematic models of BMP7 and TGFβ signaling pathways in thermogenesis. BMP7 binds TGFβR, which activates SMAD1/5/8, leading to expression of adipogenic and thermogenic genes as well as suppression of Pref1 and Wnt10a in precursor cells to promote brown and beige adipogenesis. In mature adipocytes, BMP7 signaling increases FA uptake and mitochondrial activity, resulting in enhanced thermogenesis. TGFβ activates SMAD2/3 that suppresses PGC1α expression and COX2/PGE2 pathway to reduce thermogenesis. See text for details. BMP7, bone morphogenetic protein 7; COX2, cyclooxygenase 2; FA, fatty acid; PGC1α, peroxisome proliferator activated receptor γ coactivator; PGE2, prostaglandin E2; Pref1, preadipocyte factor 1; SMAD, mothers against decapentaplegic homolog; TβR1, TGFβ receptor 1; TGFβ, Transforming growth factor beta; TGFβR, TGFβ receptor; WNT10a, Wnt family member 10A.

Chapter 2
Apold1 is a novel activator of thermogenesis in brown adipocytes

Apold1 is a novel activator of thermogenesis in brown adipocytes

Abstract

Despite its beneficial effects on metabolism, the mechanism of brown adipose tissue (BAT) thermogenesis is not fully understood. Here, we utilized CRISPR-Cas9 screening to identify and characterize novel regulators of thermogenesis. We found Apold1 to be highly enriched in BAT and induced upon various β_3-adrenergic stimuli. Gain- and loss-of-function experiments *in vitro* confirmed that Apold1 promotes thermogenesis. Lentivirus injection of Apold1 into BAT increased cold tolerance and oxygen consumption in mice. Thus, we demonstrate that Apold1 plays a critical role in promoting thermogenesis, which could be explored as a new therapeutic avenue against obesity and type 2 diabetes.

Introduction

Obesity, which is characterized by excess white adipose tissue (WAT) accumulation, has become a global health issue as it is a risk factor for a variety of diseases including diabetes and cardiovascular diseases (Caballero 2007; Goran, Ball, and Cruz 2003). While WAT stores excess energy as fat, brown adipose tissue (BAT) plays a critical role in increasing energy expenditure through thermogenesis, where it dissipates heat by burning fuels such as fat and glucose (Nedergaard and Cannon 2018). Additionally, beige adipocytes arise in white adipose depots upon certain stimuli such as cold exposure (called browning or beiging) and exhibit thermogenic capacity similar to that of brown adipocytes (Wu et al. 2012). Although there are currently no effective treatments for obesity other than lifestyle changes, the recent findings of active brown or brown-like adipose tissue in adult humans presented increasing BAT thermogenesis as an attractive strategy to combat obesity and its comorbidities (Mauro et al. 2008; Nedergaard, Bengtsson, and Cannon 2007). Indeed, both BAT mass and BAT activity inversely correlate with BMI in adult humans (Cypess et al. 2009; van Marken Lichtenbelt et al. 2009). Furthermore, BAT activation improves metabolic parameters such as glucose homeostasis and insulin sensitivity (Q. Wang et al. 2015; Chondronikola et al. 2014).

Brown and beige adipocytes highly express uncoupling protein 1 (UCP1) to perform thermogenesis (Ikeda and Yamada 2020). UCP1 is localized in the mitochondrial inner membrane and transports protons from the intermembrane space to the matrix to generate heat, resulting in uncoupling of proton gradients from ATP synthesis. Upon cold exposure, norepinephrine is released and binds β_3-adrenergic receptors in adipose tissues, leading to PKA activation (Tabuchi and Sul 2021). PKA in turn activates many downstream factors to promote lipolysis and transcription of thermogenic and mitochondrial genes such as UCP1 and PGC1α, respectively. Lipolysis produces fatty acids which not only are used as substrates for thermogenesis but also directly activate UCP1 (Fedorenko, Lishko, and Kirichok 2012). Regardless, whether there are other factors regulating thermogenesis is yet to be known.

Here, we performed CRISPR-Cas9 screening in brown adipocytes in an attempt to identify such novel thermogenic activators. Out of the 6 top candidates that were examined,

Apold1 showed the greatest increase in response to cold exposure in BAT. Apold1 also has multiple GWAS indications in metabolism and highest expression in BAT among other tissues. In fact, CRISPR Apold1 KO cells showed reduced thermogenesis while Apold1 overexpression increased thermogenesis. Moreover, lentivirus overexpression of Apold1 in BAT increased oxygen consumption rate as well as body temperature during cold challenge, highlighting the role of Apold1 in promoting thermogenesis.

Results

CRISPR-Cas9 screening identified Apold1 as a potential thermogenic activator

In order to identify novel thermogenic activators, we performed genome-wide CRISPR-Cas9 screening with a library containing 250,000 gRNAs. Stable Cas9-expressing cell line was established by traducing preadipocytes with Cas9 lentivirus followed by blasticidin selection (Figure 1A-B). We confirmed that Cas9 integration did not affect the differentiation ability of the cells by Oil Red O staining (Figure 1C). The gRNA library was then packaged into lentivirus and used to transduce the Cas9-expressing preadipocytes. After hygromycin selection of gRNA-positive cells, the cells were differentiated into mature brown adipocytes. Mature brown adipocytes were then stained with ERthermAC, which inversely correlates with the levels of thermogenesis (Kriszt et al. 2017). During the cell sorting, we first selected properly differentiated cells based on the side scatter, which reflects the accumulation of lipid droplets inside the cell, and then collected the 1% of the population with the lowest levels of thermogenesis based on the ERthermAC staining (Y.-H. Lee et al. 2004) (Figure 1D). Next generation sequencing revealed the very top hit as Ndufs3, the core subunit of mitochondrial complex I, which most definitely affects thermogenesis and therefore serves as a positive control for this screening (Figure 1E). In order to evaluate the other top candidate genes that also had 3 different gRNAs enriched, we examined the expression levels in different tissues. 2 out of the 6 candidate genes, apolipoprotein L domain-containing protein 1 (Apold1) and CKLF-like MARVEL transmembrane domain-containing protein 4 (Cmtm4) had the highest expression in BAT among the tissues tested (Figure 1F). We also asked if any genes respond to cold exposure in BAT. Indeed, Apold1 exhibited more than 10-fold increase in mRNA levels upon cold exposure (Figure 1G). Furthermore, Apold1 shows association with various metabolic traits on GWAS such as BMI-adjusted or non-adjusted waist-hip ratio, BMI-adjusted hip circumference and birth weight (Figure 1H). Altogether, we found Apold1 to be the most promising candidate gene as a thermogenic activator and decided to perform further investigation.

Apold1 is enriched in brown adipocytes and induced by β_3-adrenergic stimuli

Apold1 contains two coiled-coil domains and two transmembrane domains (Figure 2A). Although it has also been described as vascular early response gene (Verge) due to its induction by stress in endothelial cells of cerebral vessels, the role of Apold1 is not fully understood and has never been investigated in adipocytes (Regard et al. 2004; F. Liu et al. 2012; Mirza et al. 2013; Diaz-Cañestro et al. 2020; Stritt et al. 2020). Since Apold1 was enriched in BAT, we

performed stromal vascular fractionation (SVF) to see in which fraction of BAT it is mostly expressed. Apold1 levels were more than 10-fold higher in adipocyte fraction indicated by Ucp1 and Fabp4 enrichment compared to stromal vascular fraction, implying its role in mature adipocytes (Figure 2B). To confirm this result *in vitro*, we differentiated preadipocytes into mature brown adipocytes. As expected, Pparγ expression increased while a preadipocyte marker, Sox9, decreased after differentiation (Figure 2C, middle and right). Apold1 mRNA levels indeed increased after differentiation, which was consistent with the above fractionation results (Figure 2C, left).

Given that Apold1 expression was greatly induced upon cold exposure in BAT, we examined if it is also induced in inguinal WAT (iWAT), which can undergo browning. Similar to Ucp1 that is induced in both BAT and iWAT, Apold1 was also induced by cold in iWAT as well, while Pparγ remained unchanged (Figure 2D). Consistent with this, Apold1 expression increased after beige differentiation of 3T3-L1 cells, indicated by an increase in a beige adipocyte marker, Tmem26 (Figure 2E). Because cold exposure/browning of iWAT is mediated by β_3-adrenergic signaling, we treated brown adipocytes with different drugs that activate β_3-adrenergic signaling. Indeed, forskolin, IBMX and isoproterenol were all able to increase Apold1 expression *in vitro* (Figure 2F). In this regard, previous studies reported that Apold1 induction peaked around 30-45 minutes and then mostly disappeared within 60 minutes in the brain (Regard et al. 2004; Roszkowski et al. 2016). However, we found that Apold1 remained induced in brown adipocytes over the course of 120 minutes (Figure 2G). We also monitored Apold1 expression *in vivo* and found that Apold1 was greatly induced as soon as 1 hour of cold exposure (Figure 2H). Although the expression somewhat decreased after 1 hour, it still remained significantly elevated compared to before cold exposure, implying the different transcriptional regulations of Apold1 in different cell types.

Finally, we examined the localization of Apold1 by overexpression in HEK293FT cells. Both immunofluorescence microscopy and cell fractionation revealed that Apold1 localized in both cytosol and plasma membrane, which is consistent with previous reports (Regard et al. 2004; Stritt et al. 2020). Taken together, these results suggest that Apold1 is likely to play a critical role in thermogenesis by responding to β_3-adrenergic stimuli in adipocytes.

Apold1 promotes thermogenesis in brown adipocytes *in vitro*

In order to validate Apold1 as a thermogenic activator, we next established Apold1 CRISPR KO cells. Genome editing of Apold1 was confirmed by mismatch cleavage assay combined with DNA gel electrophoresis (Figure 3A). ERthermAC staining followed by flow cytometry analysis revealed that Apold1 KO had reduced thermogenesis as ERthermAC inversely correlates with thermogenesis (Figure 3B). We next measured oxygen consumption rate (OCR) by Seahorse Analyzer as another indicator for thermogenesis. We found that Apold1 KO cells had lower OCR under all conditions tested including uncoupled OCR after oligomycin treatment, which usually reflects UCP1-mediated thermogenesis (Figure 3C). In addition, mitochondrial depolarization of the KO cells were examined using JC-1 dye, which emits red

fluorescent as dimers without depolarization while it becomes monomers with green fluorescent upon depolarization. Apold1 KO cells had increased red/green ratio, indicating reduced mitochondrial depolarization and thus thermogenesis (Figure 3D).

Next, we overexpressed Apold1 in brown adipocytes (Figure 3E). Apold1 overexpression resulted in reduced ERthermAC intensity, similarly to forskolin treatment that also reduces the intensity, meaning Apold1 increased thermogenesis (Figure 3F). Uncoupled OCR was also higher in Apold1-overexpressing cells (Figure 3G). Of note, neither knockout or overexpression of Apold1 affected the differentiation of the cells as seen by the degree of lipid droplet accumulation (data not shown). These results demonstrate that Apold1 promotes thermogenesis in brown adipocytes.

Apold1 increases body temperature and oxygen consumption in mice

In an effort to determine the effect of Apold1 *in vivo*, we obtained Apold1 whole body knockout mice from Worley Lab in Johns Hopkins University. Unexpectedly, the KO mice exhibited lower body weight compared to WT mice (Figure 4A). We reasoned this might be due to altered food intake regulation since Apold1 is also expressed in the brain (Regard et al. 2004; Roszkowski et al. 2016). We found that the KO mice indeed ate less food compared to the WT, which explains the reduced weight of the KO mice and therefore makes the whole body KO mice inappropriate for our study (Figure 4B).

To assess the BAT-specific role of Apold1, we next injected Apold1 lentivirus into BAT. Apold1 was overexpressed more than 3-fold compared to empty vector (EV)-injected mice (Figure 4C). After 6 hours of cold exposure, Apold1-injected mice had higher body temperature, implying the role of Apold1 in promoting thermogenesis (Figure 4D). We then measured the oxygen consumption using CLAMS. Apold1-injected mice had significantly higher oxygen consumption during thermoneutral night, room temperature day and cold temperature night (Figure 4F). Of note, food intake of Apold1-injected mice was not different from that of EV-injected mice (Figure 4E). Interestingly, Apold1-injected BAT had higher mRNA expression of a couple thermogenic genes, Ucp1 and Nrf1, although whether this is a direct or indirect effect requires further investigation (Figure 4G). Altogether, these data suggest that Apold1-overexpression in BAT increases body temperature and oxygen consumption in mice.

Discussion

Recent discoveries of active BAT in human adults has brought enormous attention to BAT as a therapeutic target for obesity, type 2 diabetes and other metabolic diseases (Nedergaard, Bengtsson, and Cannon 2007; McNeill, Suchacki, and Stimson 2021). BAT produces heat mainly through UCP1, whose function and transcription are activated by β_3-adrenergic signaling (Tabuchi and Sul 2021). β_3-adrenergic signaling also upregulates the transcription of other thermogenic genes and mitochondrial genes in order to maximize thermogenesis. Additionally, substrate cycling such as SERCA2b-mediated calcium cycling, creatine-phosphocreatine cycling, and triglyceride-fatty acid cycling are also proposed to

generate heat (Chouchani, Kazak, and Spiegelman 2018; Ikeda and Yamada 2020). Regardless of whether UCP1-dependent mechanism or not, we sought to identify novel thermogenesis activators in brown adipocytes by utilizing genome-wide CRISPR-Cas9 screening combined with a direct, temperature sensitive-dye, ERthermAC (Kriszt et al. 2017). We found that the top hit was Ndufs3, the core subunit of the mitochondrial complex I, serving as a positive control for this screening. We then investigated the following 6 genes that also had 3 different gRNAs detected with high abundance. Based on the cold induction in BAT, tissue expression and GWAS data, we chose Apold1 as the most promising thermogenic candidate to follow up on.

Apold1 is a poorly characterized protein, originally named as vascular early response gene, Verge, since it was immediately induced by seizure in endothelial cells of cerebral vessels (Regard et al. 2004). A handful of studies have been done since then mostly in endothelial cells or the brain, reporting that Apold1 deficiency caused endothelial dysfunction, worsened stroke outcomes, or was associated with arterial thrombosis (F. Liu et al. 2012; Mirza et al. 2013; Roszkowski et al. 2016; Stritt et al. 2020; Diaz-Cañestro et al. 2020). However, these studies do not provide much mechanistic insights and how Apold1 works remains elusive, in addition to no study ever done in adipocytes. Based on the sequence, Apold1 possesses two coiled coil domains and two transmembrane domains, which are usually important for protein-protein interaction and membrane insertion, respectively. Apold1 has multiple ATTTA mRNA instability signals in the 3' UTR and one ubiquitination site at K260 in its protein sequence, implying the tight regulation of Apold1 levels both at mRNA and protein levels.

Apold1 expression was higher in BAT adipocyte fraction, increased after both brown and beige adipocyte differentiation, and inducible in both BAT and iWAT upon cold exposure. Treatments by isoproterenol, IBMX and forskolin confirmed that β_3-adrenergic signaling induces Apold1 expression, strongly indicating the importance of Apold1 in thermogenesis. Loss- and gain-of function experiments *in vitro* showed that Apold1 increases intracellular temperature and oxygen consumption. Consistently, injecting Apold1 into BAT made the mice more cold tolerant and increased the oxygen consumption of the mice, highlighting the physiological role of Apold1 in BAT. Lastly, immunofluorescence microscopy and plasma membrane extraction revealed that Apold1 localizes on the plasma membranes as well as in the cytosol. It would be interesting to see if it promotes thermogenesis by promoting β_3-adrenergic signaling, starting with measuring cAMP levels upon overexpression and/or knockdown of Apold1, since it reflects β_3-adrenergic receptor activation and the subsequent adenylate cyclase activity on the plasma membrane.

Regardless, Apold1 is a novel thermogenic gene that is highly expressed in brown adipocytes. Since Apold1 is also found in beige adipocytes as well, understanding and leveraging the role of Apold1 will be the key to fight obesity in human adults, who some claim have beige adipocytes rather than brown adipocytes.

Experimental Procedures

Animals

All protocols for mice studies were approved from the University of California at Berkeley Animal Care and Use Committee. Mice were fed a chow diet *ad libitum*. Oxygen consumption was measured using the Comprehensive Laboratory Animal
Monitoring System. Data were normalized to lean body mass measured by EcoMRI. Body temperatures were assessed using a RET-3 rectal probe for mice (Physitemp).

Cell Cultures and Stainings

Brown adipocyte cell line was obtained from Kajimura Lab (formerly at UCSF, now at Harvard). BAT cells and HEK293FT cells were maintained in DMEM containing 10% FBS and 1% pen/strep prior to differentiation/transfection. Brown adipocyte differentiation was induced with insulin (5μg/ml), T3 (1nM), rosiglitazone (0.5μM), IBMX (0.5mM), dexamethasone (2μg/ul) and indomethacin (125μM) for 48hrs and then maintained with insulin (5μg/ml), T3 (1nM) and rosiglitazone (0.5μM) for another 48hrs. On day4, differentiated cells were treated with forskolin (10μM), IBMX (0.5mM) or isoproterenol (10μM) for 6 hrs before downstream applications. For Oil Red O staining, differentiated cells were washed once with phosphate-buffered saline and subsequently fixed for 30 minutes in 4% paraformaldehyde. Cells were incubated in 60% isopropanol then stained with Oil Red O working solution for 1 hour. Cells were washed twice with distilled water prior to visualization. For ERthermAC and JC-1 staining, differentiated cells were trypsinized, resuspended in the maintenance media with 125nM ERthermAC or 2μM JC-1 and then incubated at room temperature for 30min on a shaker wrapped with aluminum foil. The cells were collected, resuspended in PBS and filtered prior to FACS analysis. For beige differentiation, 3T3-L1 cells were differentiated with the same induction cocktail described above for 48 hours and then with the maintenance media for 48-96 hours. For CRISPR KO cells, CAS9 Blasticidin Lenti Particles (LVCAS9BST, Sigma) were infected with brown preadipocytes, followed by blasticidin selection. The gRNA was packaged into lentivirus using MISSION® Lentiviral Packaging Mix (SHP001, sigma), which was used to transduce the Cas9 cells. The gRNA positive cells were then selected with Hygromycin. CRISPR editing was confirmed by Alt-R® Genome Editing Detection Kit (#1075931, IDT). For immunofluorescence, cells were grown/plated on FBS-coated coverglass in 12-well plate, washed with PBS once, fixed with 4% PFA/PBS for 10 minutes, permeabilized with 0.2% Triton/PBS for 5 minutes, and washed with PBS twice before blocking with filtered 1% BSA/PBS for 30 minutes at room temperature. Primary antibody incubation was performed at 4C overnight, followed by two washes and secondary antibody incubation at room temperature for 1 hour. After another two washes, the coverglass was mounted with Duolink® In Situ Mounting Medium with DAPI (DUO82040-5ML, Sigma) before imaging with LSM710.

RNA Isolation and RT-qPCR

Total RNA was isolated using TRIzol reagent (Invitrogen), followed by cDNA synthesized by SuperScript II (Invitrogen) using 500 ng of the isolated RNA. qPCR was then performed with

BioRad CFX96 Touch Real Time PCR (BioRad). Statistical analysis of the qPCR was obtained using the ΔΔCt method with eef1a1 as the control. Primer sets used are listed in Table 1.

Western Blotting and Plasma Membrane Extraction

Cells or tissues were lysed in 1X Cell Lysis Buffer (Cell Signaling) for 20min on ice. For tissues, TissueLyser II (QIAGEN) was also used. Lysates were then spun down for 10 min at 4℃ at 21,130g to remove the insoluble pellet. Proteins were separated by SDS-PAGE, transferred to nitrocellulose membrane and probed with the indicated antibodies in EveryBlot Blocking Buffer (BioRad). Plasma membrane extraction was performed using Plasma Membrane Protein Extraction Kit (ab65400, abcam) prior to western blotting. Antibodies used are listed in Table 2.

Stromal Vascular Fractionation

Tissues were harvested from mice, diced with scissors and incubated in 1mg/ml collagenase in 3% BSA/HBSS at 37℃ for 40 minutes. The digested tissues were then spun down at 800g for 5min and the adipocyte layer was collected. The cell pellet was resuspended in 5ml of 3% BSA/HBSS and filtered through a 100μm strainer. The flow-through was spun down at 800g for 5 minutes, the pellet was resuspended in 5ml of 3% BSA/HBSS again, and filtered through 70μm and 40μm strainers sequentially. The final flow-through was spun at 800g for 5min and the pellet was incubated in 1X Red Blood Cell Lysis Buffer on ice for 10min on a shaker, which was subsequently spun down to collect stromal vascular fraction.

Seahorse Assay

BAT cell line cells were differentiated in 12-well plates, trypsinized, and reseeded in XF24 plates at 50K cells per well at day 3 of differentiation and assayed on day 4 of differentiation. On the day of experiments, the media was replaced with XF-DMEM (Sigma-Aldrich) supplemented with 1 mM sodium pyruvate and 17.5 mM glucose and the cells were then incubated for 1 hour at 37℃ without CO_2 prior to analysis on the XF24 Analyzer. During the assay, 1mM oligomycin, 1 mM FCCP and 1mM of Rotenone/Antimycin A were added to the cells in order.

Acknowledgements

The work was supported in part by NIDDK grant to H.S.S. The authors declare no competing financial interests.

References

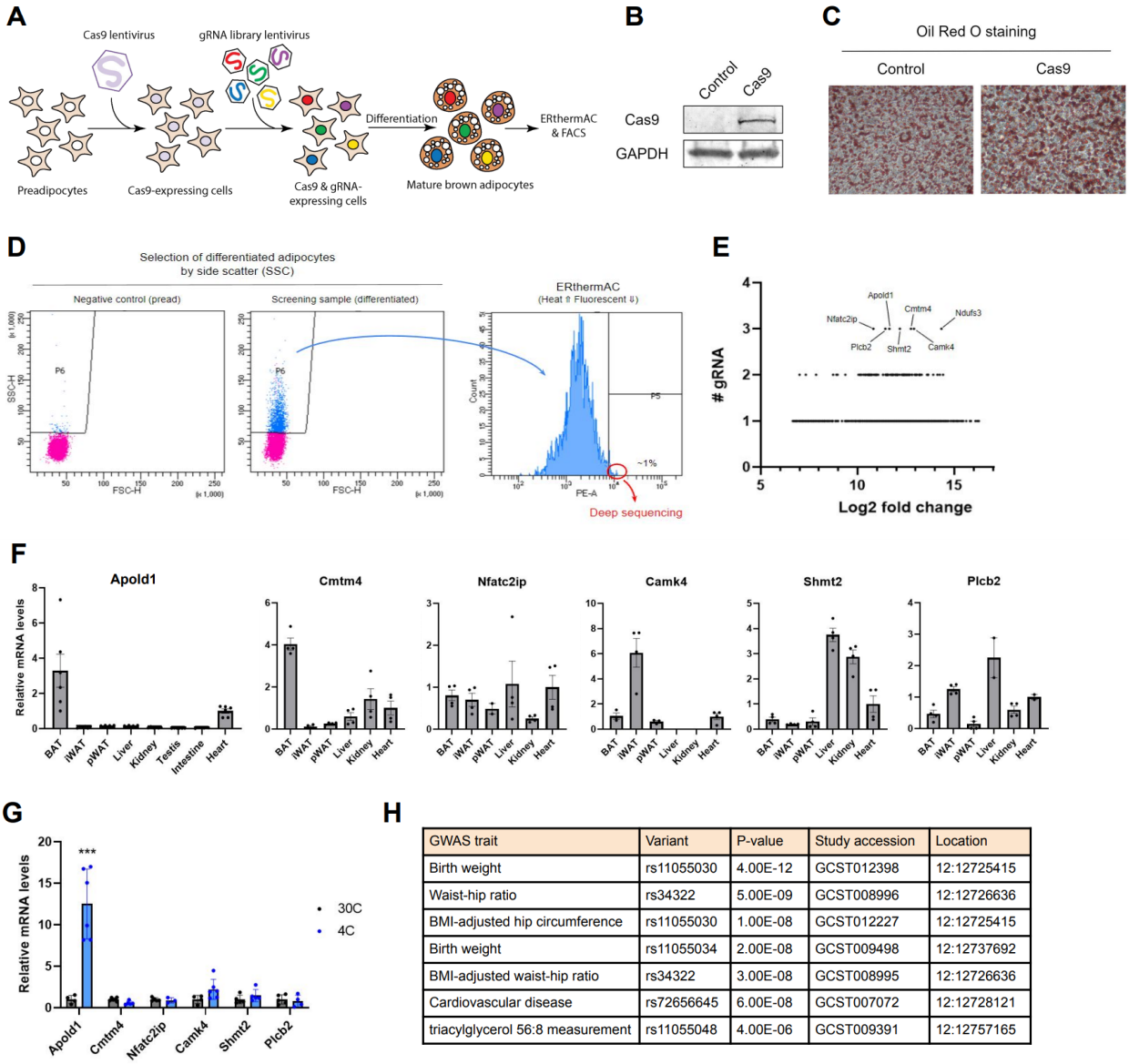
Caballero, Benjamin. 2007. “The Global Epidemic of Obesity: An Overview.” *Epidemiologic Reviews* 29 (June): 1–5.

Chondronikola, Maria, Elena Volpi, Elisabet Børsheim, Craig Porter, Palam Annamalai, Sven Enerbäck, Martin E. Lidell, et al. 2014. “Brown Adipose Tissue Improves Whole-Body Glucose Homeostasis and Insulin Sensitivity in Humans.” *Diabetes* 63 (12): 4089–99.

Chouchani, Edward T., Lawrence Kazak, and Bruce M. Spiegelman. 2018. “New Advances in

Adaptive Thermogenesis: UCP1 and Beyond." *Cell Metabolism*, November. https://doi.org/10.1016/j.cmet.2018.11.002.
Cypess, Aaron M., Sanaz Lehman, Gethin Williams, Ilan Tal, Dean Rodman, Allison B. Goldfine, Frank C. Kuo, et al. 2009. "Identification and Importance of Brown Adipose Tissue in Adult Humans." *The New England Journal of Medicine* 360 (15): 1509–17.
Diaz-Cañestro, Candela, Nicole R. Bonetti, Patricia Wüst, Vanasa Nageswaran, Luca Liberale, Jürg H. Beer, Fabrizio Montecucco, Thomas F. Lüscher, Johannes Bohacek, and Giovanni G. Camici. 2020. "Apold1 Deficiency Associates with Increased Arterial Thrombosis in Vivo." *European Journal of Clinical Investigation* 50 (2): e13191.
Fedorenko, Andriy, Polina V. Lishko, and Yuriy Kirichok. 2012. "Mechanism of Fatty-Acid-Dependent UCP1 Uncoupling in Brown Fat Mitochondria." *Cell* 151 (2): 400–413.
Goran, Michael I., Geoff D. C. Ball, and Martha L. Cruz. 2003. "Obesity and Risk of Type 2 Diabetes and Cardiovascular Disease in Children and Adolescents." *The Journal of Clinical Endocrinology and Metabolism* 88 (4): 1417–27.
Ikeda, Kenji, and Tetsuya Yamada. 2020. "UCP1 Dependent and Independent Thermogenesis in Brown and Beige Adipocytes." *Frontiers in Endocrinology* 11 (July): 498.
Kriszt, Rókus, Satoshi Arai, Hideki Itoh, Michelle H. Lee, Anna G. Goralczyk, Xiu Min Ang, Aaron M. Cypess, et al. 2017. "Optical Visualisation of Thermogenesis in Stimulated Single-Cell Brown Adipocytes." *Scientific Reports* 7 (1): 1383.
Lee, Ying-Hue, Su-Yin Chen, Rudolf J. Wiesner, and Yi-Feng Huang. 2004. "Simple Flow Cytometric Method Used to Assess Lipid Accumulation in Fat Cells." *Journal of Lipid Research* 45 (6): 1162–67.
Liu, Fudong, L. Christine Turtzo, Jun Li, Jean Regard, Paul Worley, Neer Zeevi, and Louise D. McCullough. 2012. "Loss of Vascular Early Response Gene Reduces Edema Formation after Experimental Stroke." *Experimental & Translational Stroke Medicine* 4 (1): 12.
Marken Lichtenbelt, Wouter D. van, Joost W. Vanhommerig, Nanda M. Smulders, Jamie M. A. F. L. Drossaerts, Gerrit J. Kemerink, Nicole D. Bouvy, Patrick Schrauwen, and G. J. Jaap Teule. 2009. "Cold-Activated Brown Adipose Tissue in Healthy Men." *The New England Journal of Medicine* 360 (15): 1500–1508.
Mauro, Marina, Valerie Taylor, Sean Wharton, and Arya M. Sharma. 2008. "Barriers to Obesity Treatment." *European Journal of Internal Medicine* 19 (3): 173–80.
McNeill, Ben T., Karla J. Suchacki, and Roland H. Stimson. 2021. "MECHANISMS IN ENDOCRINOLOGY: Human Brown Adipose Tissue as a Therapeutic Target: Warming up or Cooling Down?" *European Journal of Endocrinology / European Federation of Endocrine Societies* 184 (6): R243–59.
Mirza, Mehwish A., Lori A. Capozzi, Yan Xu, Louise D. McCullough, and Fudong Liu. 2013. "Knockout of Vascular Early Response Gene Worsens Chronic Stroke Outcomes in Neonatal Mice." *Brain Research Bulletin* 98 (September): 111–21.
Nedergaard, Jan, Tore Bengtsson, and Barbara Cannon. 2007. "Unexpected Evidence for Active Brown Adipose Tissue in Adult Humans." *American Journal of Physiology. Endocrinology and Metabolism* 293 (2): E444–52.
Nedergaard, Jan, and Barbara Cannon. 2018. "Brown Adipose Tissue as a Heat-Producing Thermoeffector." *Handbook of Clinical Neurology* 156: 137–52.
Regard, Jean B., Sigrid Scheek, Talaibek Borbiev, Anthony A. Lanahan, Armin Schneider, Anna-Maria Demetriades, Holger Hiemisch, Carol A. Barnes, Alexander D. Verin, and Paul

F. Worley. 2004. “Verge: A Novel Vascular Early Response Gene.” *The Journal of Neuroscience: The Official Journal of the Society for Neuroscience* 24 (16): 4092–4103.
Roszkowski, Martin, Francesca Manuella, Lukas von Ziegler, Gonzalo Durán-Pacheco, Jean-Luc Moreau, Isabelle M. Mansuy, and Johannes Bohacek. 2016. “Rapid Stress-Induced Transcriptomic Changes in the Brain Depend on Beta-Adrenergic Signaling.” *Neuropharmacology* 107 (August): 329–38.
Stritt, Simon, Paquita Nurden, Alan T. Nurden, Jean-François Schved, Jean-Claude Bordet, Maguelonne Roux, Marie-Christine Alessi, David-Alexandre Trégouët, Taija Mäkinen, and Muriel Giansily-Blaizot. 2020. “Apold1 Loss Causes Endothelial Dysfunction Involving Cell Junctions, Cytoskeletal Architecture, and Weibel-Palade Bodies, While Disrupting Hemostasis.” *Haematologica*. https://doi.org/10.3324/haematol.2022.280816.
Tabuchi, Chihiro, and Hei Sook Sul. 2021. “Signaling Pathways Regulating Thermogenesis.” *Frontiers in Endocrinology* 12 (March): 595020.
Wang, Qidi, Min Zhang, Min Xu, Weiqiong Gu, Yun Xi, Lu Qi, Biao Li, and Weiqing Wang. 2015. “Brown Adipose Tissue Activation Is Inversely Related to Central Obesity and Metabolic Parameters in Adult Human.” *PloS One* 10 (4): e0123795.
Wu, Jun, Pontus Boström, Lauren M. Sparks, Li Ye, Jang Hyun Choi, An-Hoa Giang, Melin Khandekar, et al. 2012. “Beige Adipocytes Are a Distinct Type of Thermogenic Fat Cell in Mouse and Human.” *Cell* 150 (2): 366–76.



H

GWAS trait	Variant	P-value	Study accession	Location
Birth weight	rs11055030	4.00E-12	GCST012398	12:12725415
Waist-hip ratio	rs34322	5.00E-09	GCST008996	12:12726636
BMI-adjusted hip circumference	rs11055030	1.00E-08	GCST012227	12:12725415
Birth weight	rs11055034	2.00E-08	GCST009498	12:12737692
BMI-adjusted waist-hip ratio	rs34322	3.00E-08	GCST008995	12:12726636
Cardiovascular disease	rs72656645	6.00E-08	GCST007072	12:12728121
triacylglycerol 56:8 measurement	rs11055048	4.00E-06	GCST009391	12:12757165

Figure 1. CRISPR-Cas9 screening identified Apold1 as a potential thermogenic activator. (A) Schematics of CRISPR-Cas9 screening in brown adipocytes. (B) Western blot analysis of Cas9 expression in Cas9-transduced cells. (C) Oil Red O staining of Cas9-expressing cells. (D) FACS analysis of the CRISPR screening cells stained with ERthermAC. (E) The screening results. (F) qRT-PCR analysis of the candidate genes in different tissues. (G) qRT-PCR analysis of the candidate genes in cold-exposed BAT. (H) GWAS data on Apold1.

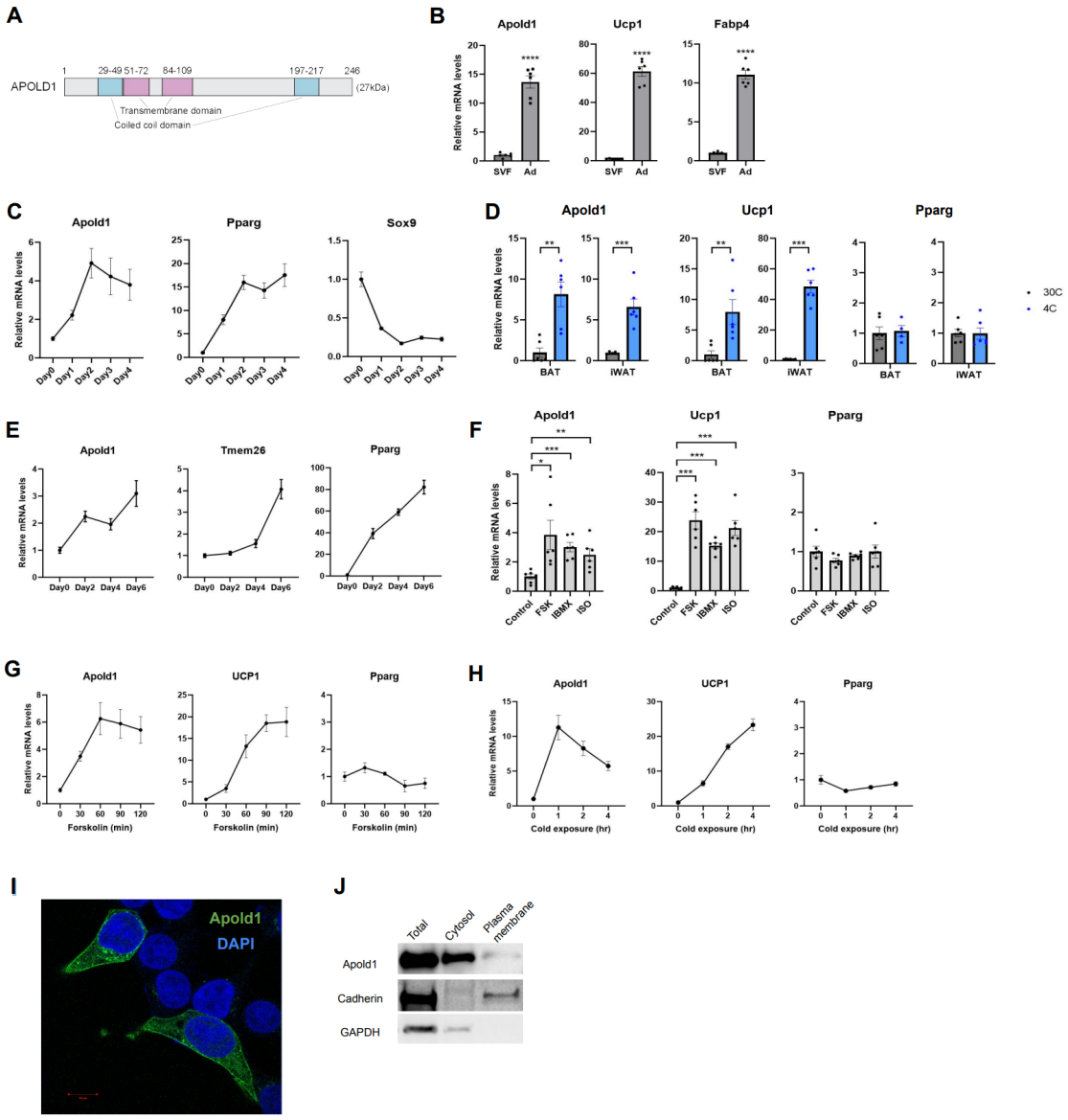


Figure 2. Characterization of Apold1.

(A) Diagram of Apold1 structure. (B) Apold1 mRNA levels in stromal vascular and adipocyte fractions of BAT. (C) Apold1 mRNA levels during brown adipocyte differentiation. (D) Apold1 mRNA levels after cold exposure in BAT and iWAT. (E) qRT-PCR analysis of the indicated genes during beging in 3T3-L1 cells. (F) qRT-PCR analysis of the indicated genes after various β_3-adrenergic stimuli. (G) qRT-PCR analysis of the indicated genes during forskolin treatment. (H) qRT-PCR analysis of the indicated genes during cold exposure in BAT. (I) Immunofluorescence of Apold1-transfected cells. (J) Plasma membrane extraction and western blot analysis of Apold1-transfected cells.

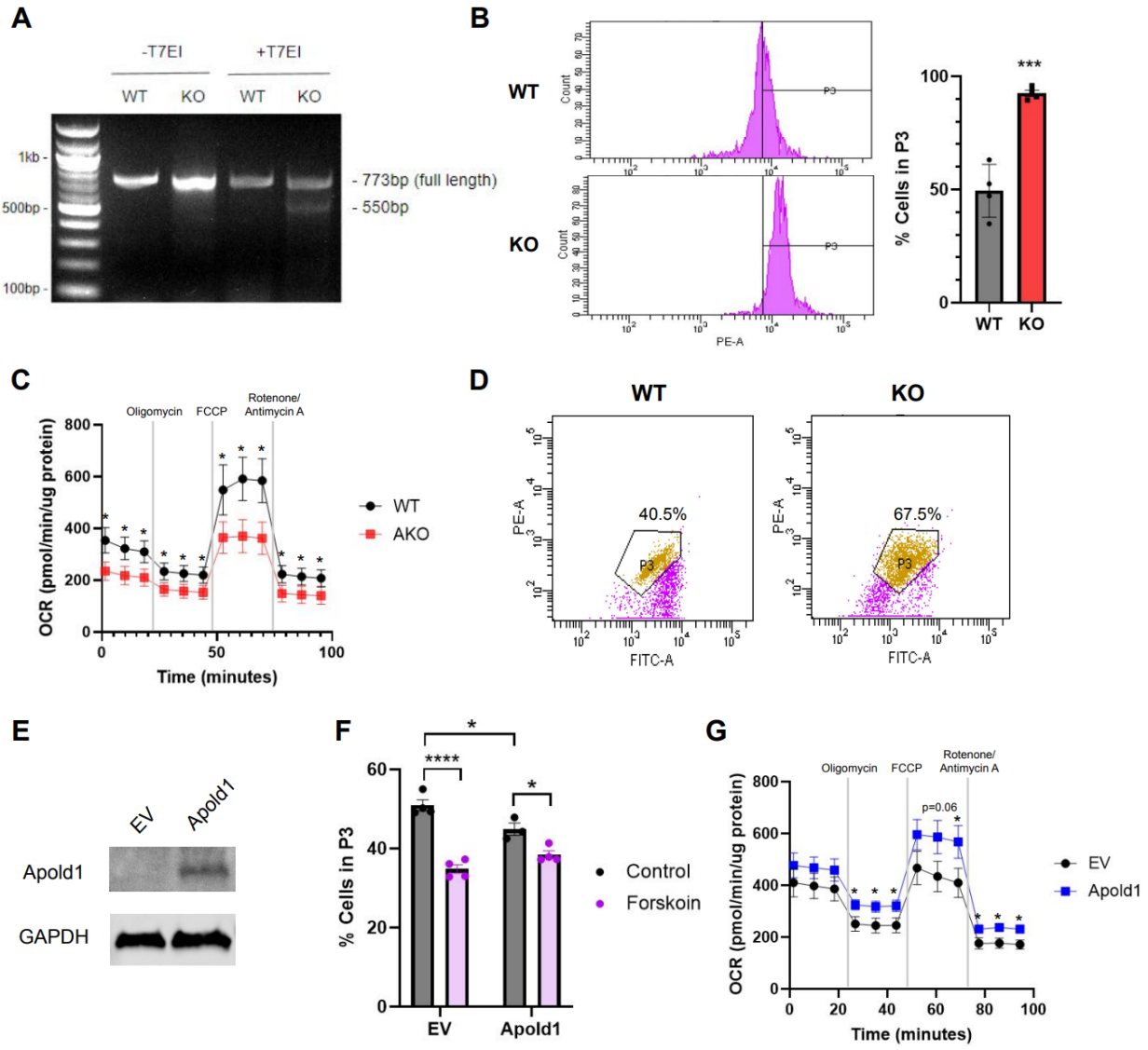


Figure 3. Apold1 gain- and loss-of-function promotes and reduces thermogenesis *in vitro*. (A) Mismatch cleavage assay with DNA electrophoresis. (B) ERthermAC staining by FACS analysis. (C) Oxygen consumption measurement using Seahorse. (D) JC-1 staining by FACS analysis. (E) Western blot analysis of Apold1. (F) Oxygen consumption measurement using Seahorse. (G) ERthermAC staining by FACS analysis.

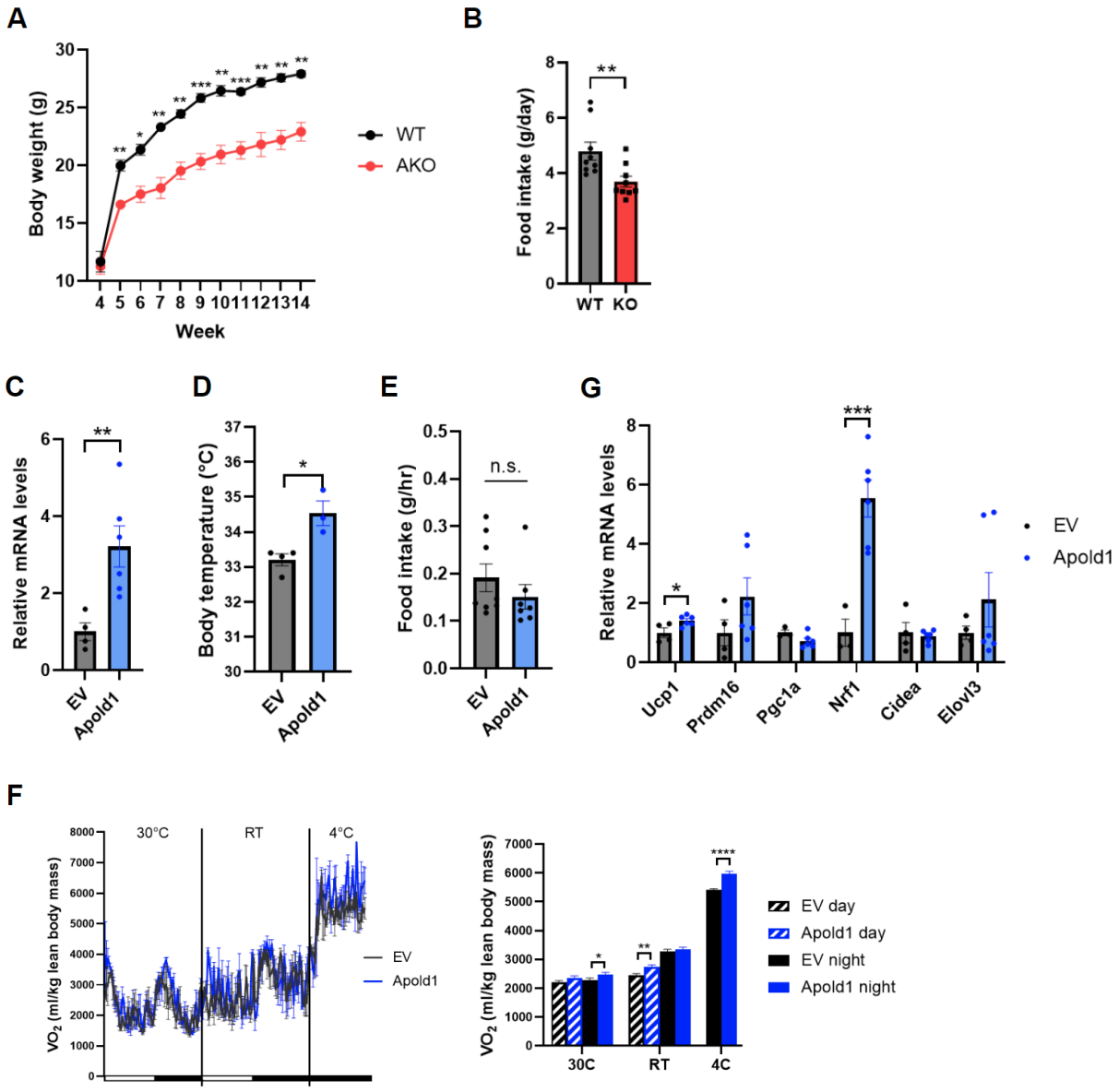


Figure 4. Characterization of Apold1 whole body knockout mice and BAT-specific overexpression mice.

(A) Body weight measurement of WT and Apold1 KO mice. (B) Food intake of WT and Apold1 KO mice. (C) qRT-PCR analysis of Apold1 in BAT of EV- or Apold1-injected mice. (D) Body temperature of EV- or Apold1-injected mice after cold exposure for 6 hours. (E) Food intake of EV- or Apold1-injected mice. (F) Oxygen consumption measurements of EV- or Apold1-injected mice. (G) qRT-PCR analysis of the indicated genes in BAT of EV- or Apold1-injected mice.

Gene	Forward	Reverse
Apold1	CCGTCCTGAAGGCCAAGATT	AGAAAAACAACGCTGCGTCC
Cmtm4	CTTTATCGCCTCAATCGTGTTGG	GTCCACATCTCTCGACTCGGT
Nfatc2ip	AGGCTCATTCCAGACACCG	GTCCTGCTCAGGTTTAGCCG
Camk4	GAGAACCTCGTCCCGGATTAC	ACACAATGGATGTAGCACCCC
Shmt2	TGGCAAGAGATACTACGGAGG	GCAGGTCCAACCCCATGAT
Plcb2	AGGATAGCTGTGATGGAAGAAGG	GCCCAGGTGTCAGGTATGTAG
Ucp1	ACTGCCACACCTCCAGTCATT	CTTTGCCTCACTCAGGATTGG
Fabp4	ACACCGAGATTTCCTTCAAACTG	CCATCTAGGGTTATGATGCTCTTCA
Pparg	AACTCTGGGAGATTCTCCTGTTGA	TGGTAATTTCTTGTGAAGTGCTCATA
Sox9	CATCAAGACGGAGCAGCTGAG	ATGGTCAGCGTAGTCGTATTG
Tmem26	ACCCTGTCATCCCACAGAG	TGTTTGGTGGAGTCCTAAGGTC
Pgc1a	ACAACGCGGACAGAATTGAG	TTCTCAAGAGCAGCGAAAGC
Nrf1	GACAAGATCATCAACCTGCCTGTAG	GCTCACTTCCTCCGGTCCTTTG
Cidea	TGCTCTTCTGTATCGCCCAGT	GCCGTGTTAAGGAATCTGCTG
Elovl3	TCCGCGTTCTCATGTAGGTCT	GGACCTGATGCAACCCTATGA
Prdm16	CAGCACGGTGAAGCCATTC	GCGTGCATCCGCTTGTG
Eef1a1	ACGAGGCAATGTTGCTGGTGAC	GTGTGACAATCCAGAACAGGAGC

Table 1. List of primers for RT-qPCR.

Protein	Catalog #	Company
GAPDH	sc-32233	Santa Cruz
Flag for WB	20543-1-AP	Proteintech
Flag for IF	14793S	Cell Signaling
E-Cadherin	14472	Cell Signaling
Apold1	PA5-82616	Invitrogen
Cas9	14697	Cell Signaling

Table 2: List of antibodies used.

Chapter 3
Rasl12 promotes thermogenesis through nuclear transport

Rasl12 may promote thermogenesis through nuclear transport

Abstract

Increasing brown adipose tissue (BAT) thermogenesis is an attractive strategy to fight metabolic diseases. Regardless, how BAT exerts thermogenesis is not fully elucidated. In order to find novel thermogenic regulators, we employed CRISPR-Cas9 screening in brown adipocytes. One of the top hits was ras-like protein family member 12 (Rasl12), which we confirmed to increase thermogenesis *in vitro* by loss-of-function and gain-of-function experiments. Rasl12 expression was the highest in BAT and responded to β_3-adrenergic simulation. We also demonstrated that Rasl12 localizes at the nuclear envelope and interacts with nuclear transport machinery. Thus, the present study provides new insights into the mechanism of BAT thermogenesis, which could help develop pharmacological strategies against obesity and T2DM.

Introduction

Obesity has become a severe worldwide epidemic, which is caused by an imbalance between energy intake and energy expenditure (Romieu et al. 2017). While white adipose tissue (WAT) stores energy as triglycerides, classical brown adipose tissue (BAT) plays an important role in energy expenditure by oxidizing fuels such as glucose and fatty acids to generate heat (Nedergaard and Cannon 2018). Recent studies showed that BAT or BAT-like tissue is present not only in rodents but also in humans and that BAT activation improves metabolic parameters (Nedergaard, Bengtsson, and Cannon 2007; Q. Wang et al. 2015). Although activation of BAT has been proposed as a strategy to combat obesity and other comorbidities, thermogenic mechanisms in BAT are not fully explored. In the present study, we utilized a genome wide loss-of-function screening using CRISPR-Cas9 system to discover and characterize novel brown adipocyte thermogenic factors.

Brown and beige adipocytes highly express uncoupling protein 1 (UCP1) for thermogenesis (Nedergaard and Cannon 2018). UCP1 is localized in the mitochondrial inner membrane and transports protons from the intermembrane space to the matrix to generate heat, resulting in uncoupling of proton gradients from ATP synthesis. Upon cold exposure, norepinephrine is released and binds β_3-adrenergic receptors in adipose tissues, leading to PKA activation (Tabuchi and Sul 2021). PKA in turn activates many downstream factors to promote lipolysis and transcription of thermogenic and mitochondrial genes such as UCP1 and PGC1α, respectively. Lipolysis produces fatty acids which not only directly activate UCP1 but also are used as substrates for thermogenesis. PGC1α promotes mitochondrial biogenesis to allow further thermogenesis. Regardless, whether there are other yet-to-be known regulators of thermogenesis is unclear.

Here, we performed CRISPR-Cas9 screening in brown adipocytes to identify such novel thermogenic activators. Rasl12 was selected as the top candidate gene to follow up as the expression was the highest in BAT and it was responsive to β_3-adrenergic stimuli. In fact, the

knockout and the overexpression cells exhibited reduced and increased thermogenesis, respectively, indicating Apold1's role in promoting thermogenesis. The contribution of Rasl12 to adipocyte thermogenesis might be through nuclear transport and/or mRNA processing as it interacts with nuclear transport machinery.

Results

CRISPR-Cas9 screening identified Rasl12 as a potential thermogenic regulator

To identify potential thermogenic activators, we utilized the CRISPR-Cas9 system with a gRNA library containing 250,000 different gRNAs. Cas9-expressing brown preadipocytes were transduced with the gRNA library, followed by the drug selection and differentiation (Figure 1A). Mature brown adipocytes were treated with forskolin to stimulate thermogenesis and stained with JC-1 as an indicator for thermogenesis. Around 10% of the cells whose mitochondria failed to depolarize after forskolin treatment were then isolated for whole genome sequencing analysis of gRNAs (Figure 1B). The top 100 genes were subjected to tissue expression analysis based on BioGPS. Among the 14 candidate genes whose expression was higher in BAT compared to most of the other tissues, we confirmed ras-like protein family member 12 (Rasl12) indeed had the highest expression in BAT by RT-qPCR and western blotting (Figure 2D-E).

Rasl12 is predicted to be a GTPase with 3 GTP binding sites, although its role has never been investigated (Figure 1C). Consistent with the tissue expression, Rasl12 was enriched in BAT adipocyte fraction compared to stromal vascular fraction (SVF) (Figure 1F). As previously reported, Sox9 was enriched in SVF whereas Pparγ and Fabp4 were highly expressed in adipocyte fraction. While Rasl12 expression was undetectable before differentiation, it increased over the course of differentiation (Figure 1G). We also observed the increased expression of Rasl12 after forskolin, isoproterenol and 8-bromo-cAMP treatment similarly to Ucp1, suggesting its responsiveness to β_3-adrenergic stimuli such as cold exposure (Figure 1H-J). In fact, Rasl12 expression increased in BAT after 1 hour of cold exposure although it decreased through 4 hours (Figure 1K). This might be because Rasl12 is especially important for the initial phase of response upon cold exposure. Alternatively, it is possible that Rasl12 protein levels might be remaining high even after mRNA levels decreased. Regardless, we found Rasl12 to be a novel, promising thermogenic activator in BAT from the CRISPR-Cas9 screening.

Rasl12 promotes thermogenesis in brown adipocytes

In order to validate the role of Rasl12 in thermogenesis, we generated a Rasl12 CRISPR KO cell line. Rasl12 mRNA levels were decreased by 70% in the KO cells (Figure 2A). ERthermAC staining, which inversely correlates with thermogenesis, showed that Rasl12 KO cells had higher intensity, indicating lower thermogenesis compared to WT (Figure 2B). Additionally, we measured oxygen consumption rate (OCR) by Seahorse Analyzer and observed that the KO cells had reduced OCR including uncoupled oxygen consumption (Figure 2C).

Next, we overexpressed Rasl12 in brown adipocytes (Figure 2D). ERthermAC staining revealed that the overexpressing cells had reduced signal intensity, indicating greater thermogenesis (Figure 2E). In accordance with this, OCR was higher in the overexpressing cells at all measurement points except after rotenone/antimycin A treatment (Figure 2F). Taken together, we demonstrate that Rasl12 promotes thermogenesis *in vitro*.

Rasl12 interacts with nuclear transporters

We then examined the localization of Rasl12 by immunofluorescence microscopy. On the contrary to GO annotation that predicts Rasl12 to be in the plasma membrane, Rasl12 was found on the nuclear envelope both in HEK293FT and BAT cells (Figure 3A). More specifically, Rasl12 was observed outside of the Lamin A/C staining, implying its localization at the outer membrane of the nuclear envelope.

In an attempt to find interacting partners of Rasl12 in BAT, we performed co-immunoprecipitation of Rasl12 followed by mass spectrometry (Figure 3B). Rasl12 was the most abundant peptide found by the mass spectrometry analysis, confirming the validity of the methods (Figure 3C). Interestingly, the vast majority of the other peptides detected were involved in mRNA processing or transport, which is consistent with the Rasl12 localization on nuclear envelope. In fact, when we co-expressed Xpo1 or Kpnb1 with RASL1 and immunoprecipitated with Rasl12, both Xpo1 and Kpnb1 were also detected, indicating their interaction with Rasl12 while the interaction with the other proteins on the list are to be determined (Figure 3D). Altogether, we show that Rasl12 localizes at nuclear envelope and is likely important for nuclear transport.

Discussion

Adipose tissue thermogenesis plays an important role in energy expenditure (Yoneshiro et al. 2011; Orava et al. 2011). Recent studies found the presence of active BAT not only in rodents but also in human adults, which presented an opportunity to target BAT to combat obesity and diabetes (Nedergaard, Bengtsson, and Cannon 2007). β_3-adrenergic signaling plays a central role in thermogenesis through activating transcription of thermogenic genes and mitochondrial genes as well as increasing substrate supply (Tabuchi and Sul 2021). However, different thermogenic mechanisms such as creatine-phosphocreatine cycling and calcium cycling have also been proposed, suggesting the presence of other thermogenic factors/mechanisms yet to be discovered (Kazak et al. 2015; Ikeda et al. 2017).

In the present study, we report the identification of a potential thermogenic factor Rasl12 through CRISPR-Cas9 screening. Rasl12 is highly expressed in BAT, specifically in adipocyte fraction compared to the stromal vascular fraction. In agreement with this, Rasl12 expression increased during differentiation *in vitro*. Another evidence that supports the role of Rasl12 in thermogenesis is that it is responsive to β_3-adrenergic stimuli only after 1 hr of cold exposure *in vivo* and forskolin, isoproterenol and 8-bromo-cAMP treatment *in vitro*. Indeed, Rasl12 CRISPR KO exhibited reduced thermogenesis while Rasl12 overexpression increased thermogenesis.

Regardless, Rasl12 expression seems to decrease eventually during cold exposure, which requires further investigation. Mass spectrometry analysis of co-immunoprecipitation experiments revealed the potential interaction between Rasl12 and nuclear transporters as well as numerous mRNA transport/processing factors. Since we were able to confirm the interaction between Rasl12 and the identified nuclear transporters, XPO1 and KPNB1, Rasl12 might promote thermogenesis by regulating nuclear import of transcription factors that are important for thermogenesis. Alternatively, Rasl12 could be regulating nuclear transport of mRNA of thermogenic genes to support thermogenesis in adipocytes.

Although we have only confirmed thus far the interaction of Rasl12 with the nuclear transport factors, it is highly possible that Rasl12 interacts with some of the other identified proteins as well. In fact, recent studies reported the regulation of alternative splicing is essential for adipocyte biology (Vernia et al. 2016; Chao et al. 2021; Chi and Lin 2018). In order to test whether Rasl12 promotes thermogenesis through regulating alternative splicing of thermogenic factors, RNA-sequencing and RT-qPCR should be performed in the RKO cells. Another way to identify potential interactions between Rasl12 and specific mRNAs is CLIP-sequencing. Ultimately, whether GTP binding ability of Rasl12 is important should be tested by mutating the GTP binding sites as well. Lastly, it would be critical to verify the function of Rasl12 in vivo by generating and characterizing BAT-specific knockout mouse and overexpression mouse models.

Experimental Procedures

Cell Cultures and Stainings

Brown adipocyte cell line was obtained from Kajimura Lab (formerly at UCSF, now at Harvard). BAT cells and HEK293FT cells were maintained in DMEM containing 10% FBS and 1% pen/strep prior to differentiation/transfection. Brown adipocyte differentiation was induced with insulin (5μg/ml), T3 (1nM), rosiglitazone (0.5μM), IBMX (0.5mM), dexamethasone (2μg/ul) and indomethacin (125μM) for 48hrs and then maintained with insulin (5μg/ml), T3 (1nM) and rosiglitazone (0.5μM) for another 48hrs. On day4, differentiated cells were treated with forskolin (10μM), IBMX (0.5mM) or isoproterenol (10μM) for 6 hrs before downstream applications. For JC-1 staining, differentiated cells were trypsinized, resuspended in the maintenance media with 2μM JC-1 and then incubated at room temperature for 30min on a shaker wrapped with aluminum foil. The cells were collected, resuspended in PBS and filtered prior to FACS analysis. For CRISPR KO cells, CAS9 Blasticidin Lenti Particles (LVCAS9BST, Sigma) were infected with brown preadipocytes, followed by blasticidin selection. The gRNA was packaged into lentivirus using MISSION® Lentiviral Packaging Mix (SHP001, sigma), which was used to transduce the Cas9 cells. The gRNA positive cells were then selected with Hygromycin. CRISPR editing was confirmed by Alt-R® Genome Editing Detection Kit (#1075931, IDT). For immunofluorescence, cells were grown/plated on FBS-coated coverglass in 12-well plate, washed with PBS once, fixed with 4% PFA/PBS for 10 minutes, permeabilized with 0.2% Triton/PBS for 5 minutes, and washed with PBS twice before blocking with filtered 1% BSA/PBS for 30 minutes at room temperature. Primary antibody incubation was performed at 4C

overnight, followed by two washes and secondary antibody incubation at room temperature for 1 hour. After another two washes, the coverglass was mounted with Duolink® In Situ Mounting Medium with DAPI (DUO82040-5ML, Sigma) before imaging with LSM710.

RNA Isolation and RT-qPCR

Total RNA was isolated using TRIzol reagent (Invitrogen), followed by cDNA synthesized by SuperScript II (Invitrogen) using 500 ng of the isolated RNA. qPCR was then performed with BioRad CFX96 Touch Real Time PCR (BioRad). Statistical analysis of the qPCR was obtained using the ΔΔCt method with eef1a1 as the control. Primer sets used are listed in Table 1.

Western Blotting

Cells or tissues were lysed in 1X Cell Lysis Buffer (Cell Signaling) for 20min on ice. For tissues, TissueLyser II (QIAGEN) was also used. Lysates were then spun down for 10 min at 4℃ at 21,130g to remove the insoluble pellet. Proteins were separated by SDS-PAGE, transferred to nitrocellulose membrane and probed with the indicated antibodies in EveryBlot Blocking Buffer (BioRad).

Stromal Vascular Fractionation

Tissues were harvested from mice, diced with scissors and incubated in 1mg/ml collagenase in 3% BSA/HBSS at 37℃ for 40 minutes. The digested tissues were then spun down at 800g for 5min and the adipocyte layer was collected. The cell pellet was resuspended in 5ml of 3% BSA/HBSS and filtered through a 100μm strainer. The flow-through was spun down at 800g for 5 minutes, the pellet was resuspended in 5ml of 3% BSA/HBSS again, and filtered through 70μm and 40μm strainers sequentially. The final flow-through was spun at 800g for 5min and the pellet was incubated in 1X Red Blood Cell Lysis Buffer on ice for 10min on a shaker, which was subsequently spun down to collect stromal vascular fraction.

Seahorse Assay

BAT cell line cells were differentiated in 12-well plates, trypsinized, and reseeded in XF24 plates at 50K cells per well at day 3 of differentiation and assayed on day 4 of differentiation. On the day of experiments, the media was replaced with XF-DMEM (Sigma-Aldrich) supplemented with 1 mM sodium pyruvate and 17.5 mM glucose and the cells were then incubated for 1 hour at 37℃ without CO_2 prior to analysis on the XF24 Analyzer. During the assay, 1mM oligomycin, 1 mM FCCP and 1mM of Rotenone/Antimycin A were added to the cells in order.

Immunoprecipitation and Mass Spectrometry Analysis

To identify interacting partners, Rasl12-myc-flag was transfected with HEK293FT cells using Lipofectamine 2000 (#11668027, ThermoFisher). 24 hours later the media was changed and another 24 hours later the cells were harvested and lysed in 1X Cell Lysis Buffer (#9803, Cell Signaling). Cell lysate was incubated with Pierce™ Anti-c-Myc Agarose (#20168,

ThermoFisher) for 1h at room temperature on a rotator. Flow-through was removed and the beads were incubated with BAT tissue lysate at 4℃ overnight. The agarose was washed with 0.1% Tween/TBS twice and eluted with 2x NuPAGE™ LDS Sample Buffer (#NP0007, ThermoFisher) by boiling for 5 minutes. The eluent was briefly run on polyacrylamide gel, the protein fraction was cut out and submitted to 1D Liquid chromatography–mass spectrometry analysis. To confirm the interaction with Xpo1 or Kpnb1, Rasl12-myc-flag was co-transfected with HA-Xpo1 or HA-Kpnb in HEK293FT cells. 200μg of cell lysate was incubated with 10ul of washed Anti-FLAG® M2 Magnetic Beads (#M8823, Sigma) or Pierce™ Anti-HA Agarose (#26181, ThermoFisher) for 1h at room temperature with rotation and after washes the eluent was obtained and run on polyacrylamide gel for western blotting.

Acknowledgements

The work was supported in part by NIDDK grant to H.S.S. The authors declare no competing financial interests.

References

Chao, Yunqi, Yonghui Jiang, Mianling Zhong, Kaiyan Wei, Chenxi Hu, Yifang Qin, Yiming Zuo, Lili Yang, Zheng Shen, and Chaochun Zou. 2021. "Regulatory Roles and Mechanisms of Alternative RNA Splicing in Adipogenesis and Human Metabolic Health." *Cell & Bioscience* 11 (1): 66.

Chi, Yi-Lin, and Jung-Chun Lin. 2018. "RBM4a Modulates the Impact of PRDM16 on Development of Brown Adipocytes through an Alternative Splicing Mechanism." *Biochimica et Biophysica Acta, Molecular Cell Research* 1865 (11 Pt A): 1515–25.

Ikeda, Kenji, Qianqian Kang, Takeshi Yoneshiro, Joao Paulo Camporez, Hiroko Maki, Mayu Homma, Kosaku Shinoda, et al. 2017. "UCP1-Independent Signaling Involving SERCA2b-Mediated Calcium Cycling Regulates Beige Fat Thermogenesis and Systemic Glucose Homeostasis." *Nature Medicine* 23 (12): 1454–65.

Kazak, Lawrence, Edward T. Chouchani, Mark P. Jedrychowski, Brian K. Erickson, Kosaku Shinoda, Paul Cohen, Ramalingam Vetrivelan, et al. 2015. "A Creatine-Driven Substrate Cycle Enhances Energy Expenditure and Thermogenesis in Beige Fat." *Cell* 163 (3): 643–55.

Nedergaard, Jan, Tore Bengtsson, and Barbara Cannon. 2007. "Unexpected Evidence for Active Brown Adipose Tissue in Adult Humans." *American Journal of Physiology. Endocrinology and Metabolism* 293 (2): E444–52.

Nedergaard, Jan, and Barbara Cannon. 2018. "Brown Adipose Tissue as a Heat-Producing Thermoeffector." *Handbook of Clinical Neurology* 156: 137–52.

Orava, Janne, Pirjo Nuutila, Martin E. Lidell, Vesa Oikonen, Tommi Noponen, Tapio Viljanen, Mika Scheinin, et al. 2011. "Different Metabolic Responses of Human Brown Adipose Tissue to Activation by Cold and Insulin." *Cell Metabolism* 14 (2): 272–79.

Romieu, Isabelle, Laure Dossus, Simón Barquera, Hervé M. Blottière, Paul W. Franks, Marc Gunter, Nahla Hwalla, et al. 2017. "Energy Balance and Obesity: What Are the Main Drivers?" *Cancer Causes & Control: CCC* 28 (3): 247–58.

Tabuchi, Chihiro, and Hei Sook Sul. 2021. "Signaling Pathways Regulating Thermogenesis."

Frontiers in Endocrinology 12 (March): 595020.
Vernia, Santiago, Yvonne Jk Edwards, Myoung Sook Han, Julie Cavanagh-Kyros, Tamera Barrett, Jason K. Kim, and Roger J. Davis. 2016. “An Alternative Splicing Program Promotes Adipose Tissue Thermogenesis.” *eLife* 5 (September). https://doi.org/10.7554/eLife.17672.
Wang, Qidi, Min Zhang, Min Xu, Weiqiong Gu, Yun Xi, Lu Qi, Biao Li, and Weiqing Wang. 2015. “Brown Adipose Tissue Activation Is Inversely Related to Central Obesity and Metabolic Parameters in Adult Human.” *PloS One* 10 (4): e0123795.
Yoneshiro, Takeshi, Sayuri Aita, Mami Matsushita, Toshimitsu Kameya, Kunihiro Nakada, Yuko Kawai, and Masayuki Saito. 2011. “Brown Adipose Tissue, Whole-Body Energy Expenditure, and Thermogenesis in Healthy Adult Men.” *Obesity* 19 (1): 13–16.

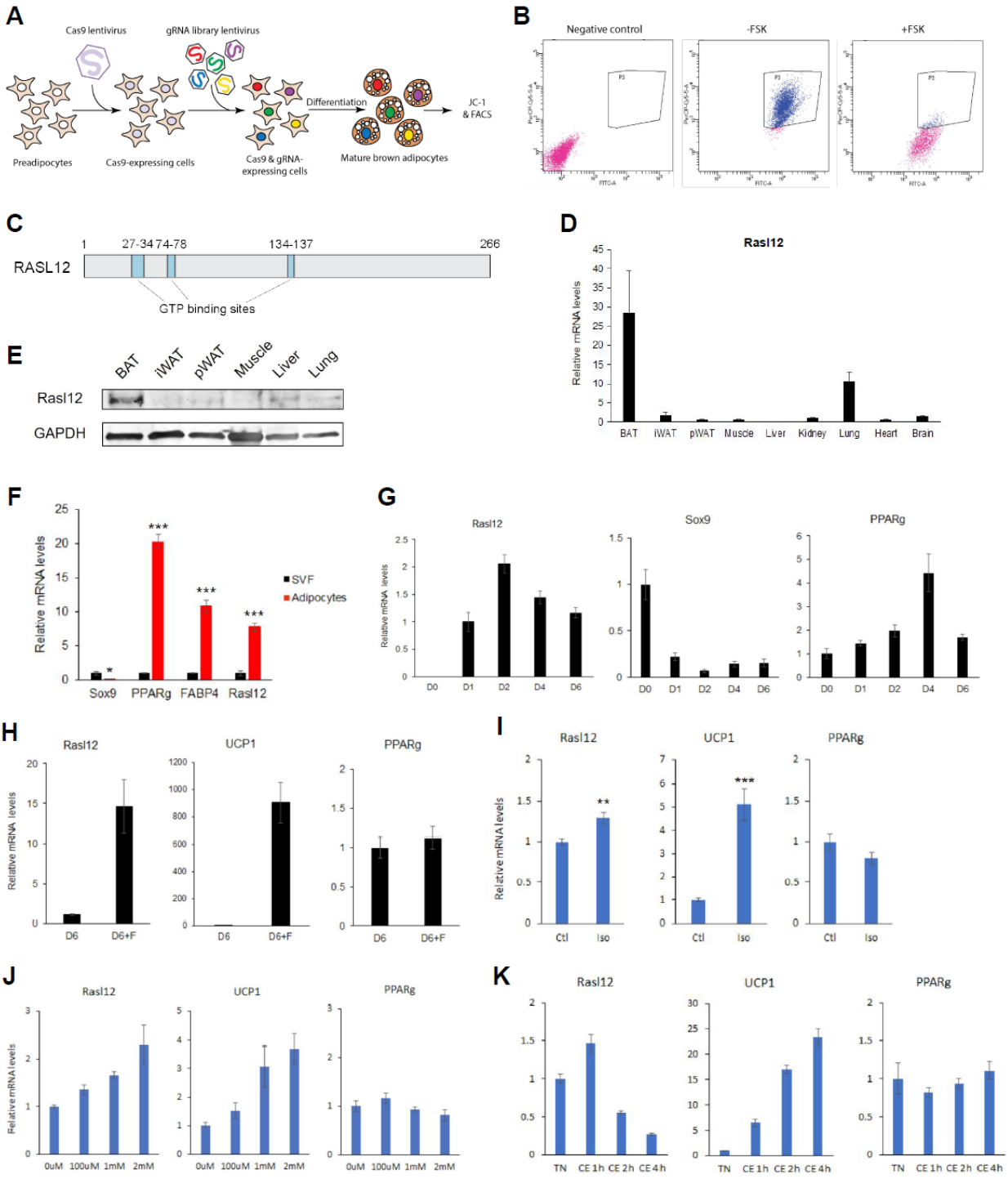


Figure 1. Identification and characterization of Rasl12.

(A) Schematics of CRISPR-Cas9 screening in brown adipocytes. (B) FACS analysis of the CRISPR screening cells stained with JC-1. (C) Diagram of Rasl12 structure. (D) qRT-PCR analysis of Rasl12 among the indicated tissues. (E) Western blot analysis of Rasl12 among the indicated tissues. (F) Stromal vascular fractionation of BAT followed by qRT-PCR for Rasl12.

(G) Rasl12 mRNA levels during brown adipocyte differentiation. (H) Rasl12 mRNA levels after forskolin treatment in brown adipocytes. (I) Rasl12 mRNA levels after isoproterenol treatment in brown adipocytes. (J) Rasl12 mRNA levels after 8-bromo-cAMP treatment in brown adipocytes. (K) Rasl12 mRNA levels during cold exposure in BAT. TN; thermoneutral, CE; cold exposure.

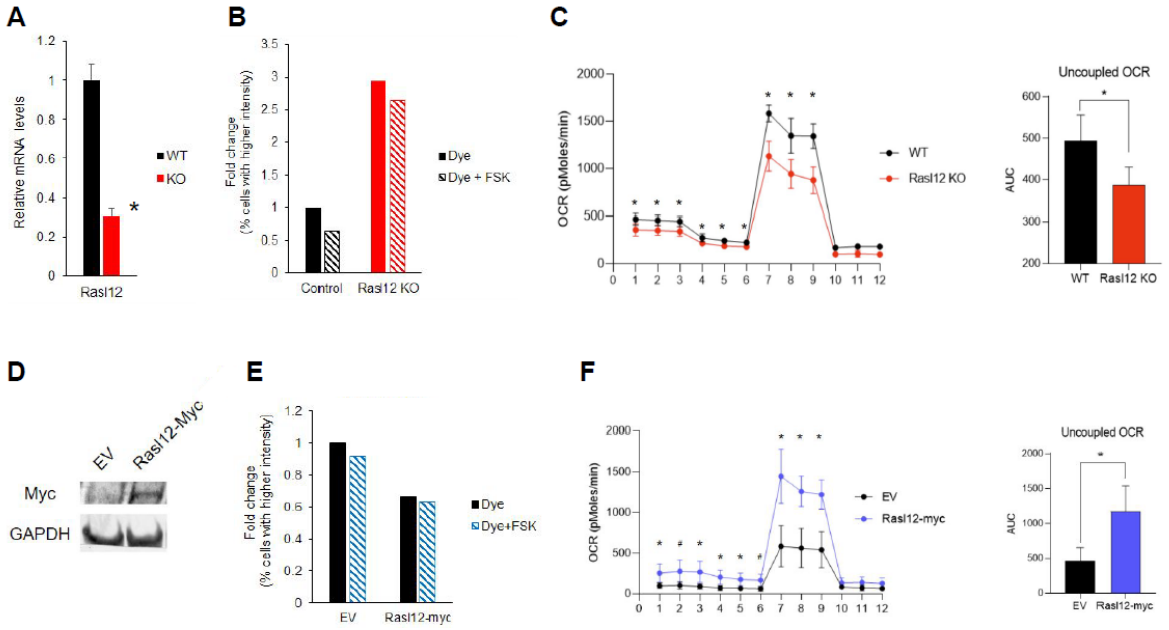
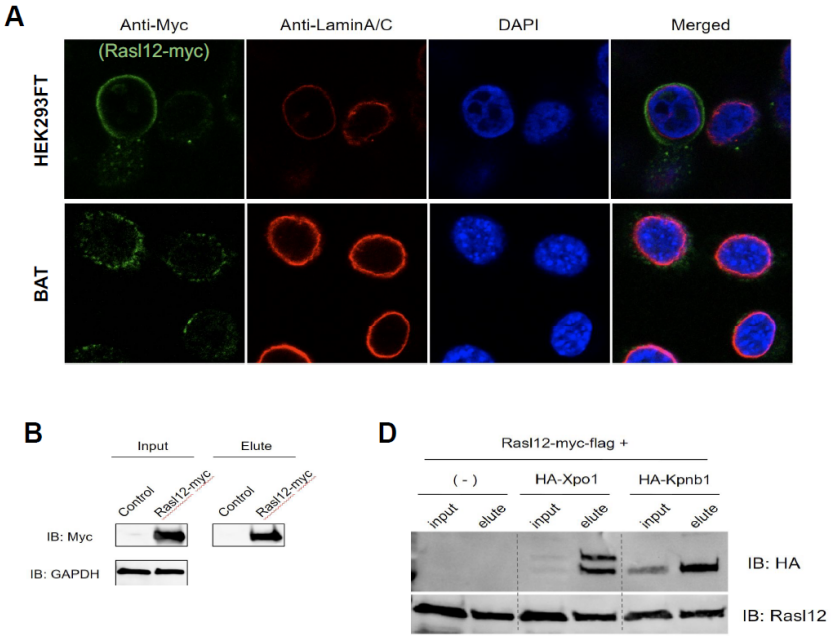


Figure 2. Rasl12 promotes thermogenesis *in vitro*.

(A) Rasl12 mRNA levels. (B) Quantification of ERthermAC^{high} cells. Dye; ERthermAC, FSK; forskolin. (C) Oxygen consumption measurement using Seahorse at day 4. Oligomycin, FCCP and rotenone/antimycin A were added after time point 3, 6, and 9, respectively. (D) Western blot of myc-tagged Rasl12. (E) Quantification of ERthermAC^{high} cells. Dye; ERthermAC, FSK; forskolin. (F) Oxygen consumption measurement using Seahorse at day 4. Oligomycin, FCCP and rotenone/antimycin A were added after time point 3, 6, and 9, respectively.



C

Sequence Count	Name		Function
16	Rasl12	ras-like protein family member 12 isoform 1	
10	Snrnp200	U5 small nuclear ribonucleoprotein 200 kDa helicase	mRNA processing
9	Prpf8	pre-mRNA-processing-splicing factor 8	mRNA processing
8	Xpo1	exportin-1	nuclear transport
7	Kpnb1	importin subunit beta-1	nuclear transport
7	Pabpc1	polyadenylate-binding protein 1	mRNA processing
6	Hnrnph2	heterogeneous nuclear ribonucleoprotein H2	mRNA processing/transport
6	Hnrnpq	heterogeneous nuclear ribonucleoprotein Q	mRNA processing/transport
6	Eif3a	eukaryotic translation initiation factor 3 subunit A	mRNA translation
5	Pabpc2	poly A binding protein, cytoplasmic 2	mRNA processing
5	Igf2bp1	insulin-like growth factor 2 mRNA-binding protein 1	mRNA transport
5	Rpl3	60S ribosomal protein L3	mRNA translation
5	Ewsr1	EWS/Ewing sarcoma breakpoint region 1	RNA-binding protein
5	Cand1	cullin-associated NEDD8-dissociated protein 1	E3 Ub ligase assembly
4	Cpsf6	cleavage and polyadenylation specificity factor subunit 6	mRNA processing
4	Srp72	signal recognition particle 72	mRNA translation
4	Brpf1	peregrin isoform 1	histone acetyltransferase subunit
4	Cad	carbamoyl-phosphate synthetase 2, aspartate transcarbamylase, and dihydroorotase	pyrimidine pathway
3	FAM120A	constitutive coactivator of PPAR-gamma-like protein 1	RNA binding, activate Src kinases
3	U2surp	U2 snRNP-associated SURP motif-containing protein isoform X2	mRNA processing

Figure 3. Rasl12 localization and potential interacting partners.
(A) Immunofluorescence. (B) Immunoprecipitation by c-Myc beads followed by western blot of the input and the eluate. (C) List of peptides found in the eluate by mass spectrometry after the immunoprecipitation. (D) Western blot analysis of co-transfection followed by co-immunoprecipitation of Rasl12 and Xpo1 or Kpnb1.

Gene	Forward	Reverse
Rasl12	CATCACCTGGTGGTAGAAAGAG	TCCAAGTGTCTTTGCCCTATC
Ucp1	ACTGCCACACCTCCAGTCATT	CTTTGCCTCACTCAGGATTGG
Fabp4	ACACCGAGATTTCCTTCAAACTG	CCATCTAGGGTTATGATGCTCTTCA
Pparg	AACTCTGGGAGATTCTCCTGTTGA	TGGTAATTTCTTGTGAAGTGCTCATA
Sox9	CATCAAGACGGAGCAGCTGAG	ATGGTCAGCGTAGTCGTATTG
Eef1a1	ACGAGGCAATGTTGCTGGTGAC	GTGTGACAATCCAGAACAGGAGC

Table 1. List of primers for RT-qPCR.

Protein	Catalog #	Company
GAPDH	sc-32233	Santa Cruz
Myc	13-2500	Invitrogen
HA	26183	Invitrogen
Rasl12	LS-C151334	LSBio
Lamin A/C	SAB4200236	Sigma

Table 2: List of antibodies used.

Chapter 4
Zc2hc1c suppresses brown adipocyte differentiation

Zc2hc1c suppresses brown adipocyte differentiation

Abstract

Although brown adipose tissue (BAT) has numerous metabolically beneficial effects, the mechanism by which the precursor cells differentiate into mature brown adipocytes remain incompletely understood. Here, we found Zc2hc1c, a novel potential repressor of brown adipocyte differentiation whose overexpression and knockout suppresses and promotes differentiation, respectively. RNA-sequencing of Zc2hc1c KO cells revealed that metabolic processes, GPCR signaling and brown adipocyte differentiation were indeed altered. Thus, Zc2hc1c inhibition will be a new therapeutic avenue as it increases BAT formation to combat obesity, T2DM and its comorbidities.

Introduction

Obesity has become a severe worldwide epidemic, which is caused by an imbalance between energy intake and energy expenditure (Romieu et al. 2017). White adipose tissue (WAT) stores energy in a form of triglycerides while classical brown adipose tissue (BAT) plays an important role in energy expenditure by oxidizing fuels such as glucose and fatty acids to generate heat (Nedergaard and Cannon 2018). Recent studies showed that BAT or BAT-like tissue is present not only in rodents but also in humans and that BAT activation in humans brings metabolically beneficial effects (Nedergaard, Bengtsson, and Cannon 2007; Q. Wang et al. 2015; Chondronikola et al. 2014). Although expansion or activation of BAT has been proposed as a strategy to combat obesity and other comorbidities, how precursor cells differentiate into mature brown adipocytes is not fully understood. Here, we found an uncharacterized protein from CRISPR-Cas9 screening, which inhibits brown adipocyte differentiation.

Brown adipocyte differentiation is carried out by a series of transcriptional regulations (Inagaki, Sakai, and Kajimura 2016). C/EBPβ is one of the transcription factors that activates the master regulator of adipogenesis, PPARγ, which in turn activates C/EBPα to synergistically promote adipocyte differentiation (Rosen et al. 2002; Madsen et al. 2014). Since C/EBPβ expression is inhibited by SOX9 in the precursor cells, SOX9 expression first needs to decrease to enable adipogenic differentiation (Y. Wang and Sul 2009). PRDM16 is another transcription factor that specifically induces brown adipocyte formation by binding PPARγ and upregulating brown fat genes such as UCP1 (Seale et al. 2008). UCP1 is the central protein for thermogenesis in brown adipocytes as it dissipates energy as heat. Upon external cues such as cold exposure, BAT β_3-adrenergic receptors are activated, causing intracellular signal transduction, leading to the upregulation of thermogenic genes as well as an increase in the substrate supply for thermogenesis (Tabuchi and Sul 2021).

Here we discovered a novel factor that suppresses brown adipocyte differentiation. The precursor cells failed to differentiate into brown adipocytes upon overexpression of Zc2hc1c. On the other hand, CRISPR KO of Zc2hc1c rendered the cells higher differentiation capacity, which was evident in the decreased expression of SOX9 and the increased expression of PPARγ,

C/EBPα, PRDM16 and FABP4 as well as increased oxygen consumption rate (OCR). RNA-sequencing further revealed that metabolic process, GPCR signaling pathway and cell differentiation were in fact altered as a result of Zc2hc1c KO.

Results

CRISPR-Cas9 screen identifies a potential repressor for brown adipocyte differentiation

In order to identify regulators for brown adipocyte differentiation, we performed a CRISPR-Cas9 screen with a gRNA library with 250,000 gRNAs. Cas9-expressing cells were first established and gRNA lentivirus was then introduced. After differentiation, we stained the cells with LipidTox and isolated LipidTox-negative cells that failed to differentiate by FACS, originally with an intention to find activators for brown adipocyte differentiation. We then followed up on the genes that are either known or predicted to be transcription factors from the list of identified genes. When we examined the expression patterns of those genes during the differentiation, we unexpectedly found that Zc2hc1c decreased, implying Zc2hc1c as a potential repressor for brown adipocyte differentiation, while no other gene changed its expression pattern during differentiation (Figure 1B).

Zc2hc1c is an uncharacterized protein that contains one coiled coil domain and one C2H2 zinc finger domain (Figure 1A). According to GWAS data, a Zc2hc1c variant is significantly associated with coronary heart disease (data not shown). Stromal vascular fractionation of BAT revealed that Zc2hc1c was enriched in stromal vascular fraction compared to adipocyte fraction (Figure 1C). Next, we overexpressed Zc2hc1c in preadipocytes and then differentiated the cells. Oil Red O (ORO) stain showed that Zc2hc1c overexpressing cells had less lipid accumulation, indicating poorer differentiation (Figure 1D). In addition, Zc2hc1c was found in the nucleus, appearing either as patches or across the nucleus depending on the cells (Figure 1E).

Zc2hc1c CRISPR KO promotes brown adipocyte differentiation

In order to further confirm the repressive role of Zc2hc1c in brown adipocyte differentiation, we generated Zc2hc1c CRISPR KO cells (ZKO). Zc2hc1c expression was indeed reduced in ZKO cells compared to wild type (WT) (Figure 2A). RT-qPCR analysis revealed that Sox9 expression decreased while Pparγ and Fabp4/aP2 expression increased in WT as previously reported (Figure 2B). In ZKO, however, Sox9 expression was significantly lower before differentiation (day 0) and remained throughout differentiation. On the other hand, Pparγ and Fabp4/aP2 expression was higher in ZKO at day 0. Although Pparγ expression decreased over the course of differentiation, it still remained at a similar level as WT in day 4. Regardless, no obvious difference was seen by ORO between WT and ZKO after differentiation with the regular differentiation cocktail (Figure 2C). We reasoned this could be due to the fact that the regular differentiation cocktail contains ample reagents to differentiate even wild type cells well and might have hidden the difference that could have been present. To overcome this problem, we decided to remove a few drugs one by one from the cocktail to visualize the potential difference. Indeed, even upon removing indomethacin, T3 and rosiglitazone ZKO still differentiated well

whereas WT only had a minimal differentiation (Figure 2D). Consistent with this, ZKO exhibited higher oxygen consumption rate (OCR) at both basal and stimulated conditions, including uncoupled OCR (Figure 2E).

Lastly, we performed RNA-sequencing with WT and ZKO before and after differentiation (Day0 and Day 4, respectively) (Figure 3A). Cebpα, Pparγ and Prdm16 were all found to be upregulated in ZKO at both Day 0 and Day 4, indicating the higher potential of differentiation in ZKO cells compared to WT (Figure 3B). GO analysis further revealed that many biological processes involved in brown adipocyte differentiation and function such as metabolic process, GPCR signaling pathway, and brown fat cell differentiation (Figure 3C). Altogether, our data highlights the repressive role of Zc2hc1c in brown adipocyte differentiation.

Discussion

Differentiation of precursor cells into mature brown adipocytes involves a cascade of transcriptional regulations. Classical brown adipocytes originate from MYF5+/PAX7+/EN1+ multipotent stem cells in the dermomyotome, which commit to brown adipocyte lineage upon EBF2 expression (Tabuchi and Sul 2021). PRDM16, through interaction with PPARγ, and BMP7 also drive brown adipocyte differentiation of the precursor cells. Committed brown precursor cells then differentiate into mature brown adipocytes through induction of adipogenic, thermogenic as well as mitochondrial genes, which are mediated by many transcription factors including, but not limited to, EBF2, CEBPβ, PPARγ, PRDM16, IRF4, ZFP516 and ZC3H10 . However, much less is known about repressive transcription factors for brown adipocyte differentiation.

Here, we discovered Zc2hc1c as a negative regulator for brown fat differentiation. Zc2hc1c is most likely a transcription factor as it possesses C2H2 zinc finger domain and localizes in the nucleus. Although RNA-sequencing revealed that CEBPα, PPARγ and PRDM16 expressions were most significantly upregulated by Zc2hc1c KO, whether any of these genes are directly regulated by Zc2hc1c requires further experiments. Thus, the future studies should include the identification of its binding sites and its direct target genes. Moreover, finding the interacting partner(s) will provide insights into the mechanism of the regulation of Zc2hc1c activity. Animal studies should also be performed by knocking out and overspressing Zc2hc1c in a BAT-specific manner. Pharmaceutical development of Zc2hc1c inhibitors will be an attractive strategy for combating obesity and metabolic diseases as it allows the expansion of BAT mass.

Experimental Procedures

Cell Cultures and Stainings

Brown adipocyte cell line was obtained from Kajimura Lab (formerly at UCSF, now at Harvard). BAT cells and HEK293FT cells were maintained in DMEM containing 10% FBS and 1% pen/strep prior to differentiation/transfection. Brown adipocyte differentiation was induced with insulin (5μg/ml), T3 (1nM), rosiglitazone (0.5μM), IBMX (0.5mM), dexamethasone (2μg/ul) and indomethacin (125μM) for 48hrs and then maintained with insulin (5μg/ml), T3 (1nM) and

rosiglitazone (0.5μM) for another 48hrs. On day4, differentiated cells were treated with forskolin (10μM) before downstream applications. For Oil Red O staining, differentiated cells were washed once with phosphate-buffered saline and subsequently fixed for 30 minutes in 4% paraformaldehyde. Cells were incubated in 60% isopropanol then stained with Oil Red O working solution for 1 hour. Cells were washed twice with distilled water prior to visualization. For LipidToxRed staining (H34476, Thermo Fisher), differentiated cells were trypsinized, resuspended in the maintenance media with LipidTox and then incubated at room temperature for 30min on a shaker wrapped with aluminum foil. The cells were collected, resuspended in PBS and filtered prior to FACS analysis. For CRISPR KO cells, CAS9 Blasticidin Lenti Particles (LVCAS9BST, Sigma) were infected with brown preadipocytes, followed by blasticidin selection. The gRNA was packaged into lentivirus using MISSION® Lentiviral Packaging Mix (SHP001, Sigma), which was used to transduce the Cas9 cells. The gRNA positive cells were then selected with Hygromycin. For immunofluorescence, cells were grown/plated on FBS-coated coverglass in 12-well plate, washed with PBS once, fixed with 4% PFA/PBS for 10 minutes, permeabilized with 0.2% Triton/PBS for 5 minutes, and washed with PBS twice before blocking with filtered 1% BSA/PBS for 30 minutes at room temperature. Primary antibody incubation was performed at 4C overnight, followed by two washes and secondary antibody incubation at room temperature for 1 hour. After another two washes, the coverglass was mounted with Duolink® In Situ Mounting Medium with DAPI (DUO82040-5ML, Sigma) before imaging with LSM710.

RNA Isolation and RT-qPCR

Total RNA was isolated using TRIzol reagent (Invitrogen), followed by cDNA synthesized by SuperScript II (Invitrogen) using 500 ng of the isolated RNA. qPCR was then performed with BioRad CFX96 Touch Real Time PCR (BioRad). Statistical analysis of the qPCR was obtained using the ΔΔCt method with eef1a1 as the control. Primer sets used are listed in Table 1. For RNA-sequencing, RNA was extracted from cells using RNeasy Mini Kit (#74106, QIAGEN) and sent out for sequencing with Illumina HiSeq 4000.

Stromal Vascular Fractionation

Tissues were harvested from mice, diced with scissors and incubated in 1mg/ml collagenase in 3% BSA/HBSS at 37℃ for 40 minutes. The digested tissues were then spun down at 800g for 5min and the adipocyte layer was collected. The cell pellet was resuspended in 5ml of 3% BSA/HBSS and filtered through a 100μm strainer. The flow-through was spun down at 800g for 5 minutes, the pellet was resuspended in 5ml of 3% BSA/HBSS again, and filtered through 70μm and 40μm strainers sequentially. The final flow-through was spun at 800g for 5min and the pellet was incubated in 1X Red Blood Cell Lysis Buffer on ice for 10min on a shaker, which was subsequently spun down to collect stromal vascular fraction.

Seahorse Assay

BAT cell line cells were differentiated in 12-well plates, trypsinized, and reseeded in XF24 plates at 50K cells per well at day 3 of differentiation and assayed on day 4 of differentiation. On the day of experiments, the media was replaced with XF-DMEM (Sigma-Aldrich) supplemented with 1 mM sodium pyruvate and 17.5 mM glucose and the cells were then incubated for 1 hour at 37℃ without CO_2 prior to analysis on the XF24 Analyzer. During the assay, 1mM oligomycin, 1 mM FCCP and 1mM of Rotenone/Antimycin A were added to the cells in order.

Acknowledgements

The work was supported in part by NIDDK grant to H.S.S. The authors declare no competing financial interests.

References

Chondronikola, Maria, Elena Volpi, Elisabet Børsheim, Craig Porter, Palam Annamalai, Sven Enerbäck, Martin E. Lidell, et al. 2014. "Brown Adipose Tissue Improves Whole-Body Glucose Homeostasis and Insulin Sensitivity in Humans." *Diabetes* 63 (12): 4089–99.

Inagaki, Takeshi, Juro Sakai, and Shingo Kajimura. 2016. "Transcriptional and Epigenetic Control of Brown and Beige Adipose Cell Fate and Function." *Nature Reviews. Molecular Cell Biology* 17 (8): 480–95.

Madsen, Maria Stahl, Rasmus Siersbæk, Michael Boergesen, Ronni Nielsen, and Susanne Mandrup. 2014. "Peroxisome Proliferator-Activated Receptor γ and C/EBPα Synergistically Activate Key Metabolic Adipocyte Genes by Assisted Loading." *Molecular and Cellular Biology* 34 (6): 939–54.

Nedergaard, Jan, Tore Bengtsson, and Barbara Cannon. 2007. "Unexpected Evidence for Active Brown Adipose Tissue in Adult Humans." *American Journal of Physiology. Endocrinology and Metabolism* 293 (2): E444–52.

Nedergaard, Jan, and Barbara Cannon. 2018. "Brown Adipose Tissue as a Heat-Producing Thermoeffector." *Handbook of Clinical Neurology* 156: 137–52.

Romieu, Isabelle, Laure Dossus, Simón Barquera, Hervé M. Blottière, Paul W. Franks, Marc Gunter, Nahla Hwalla, et al. 2017. "Energy Balance and Obesity: What Are the Main Drivers?" *Cancer Causes & Control: CCC* 28 (3): 247–58.

Rosen, E., Chung-Hsin Hsu, Xinzhong Wang, S. Sakai, M. Freeman, F. Gonzalez, and B. Spiegelman. 2002. "C/EBP Induces Adipogenesis through PPAR: A Unified Pathway." https://www.semanticscholar.org/paper/4a13cfd3d62ebc8d7f9c099c0436af14589ed26b.

Seale, Patrick, Bryan Bjork, Wenli Yang, Shingo Kajimura, Sherry Chin, Shihuan Kuang, Anthony Scimè, et al. 2008. "PRDM16 Controls a Brown Fat/skeletal Muscle Switch." *Nature* 454 (7207): 961–67.

Tabuchi, Chihiro, and Hei Sook Sul. 2021. "Signaling Pathways Regulating Thermogenesis." *Frontiers in Endocrinology* 12 (March): 595020.

Wang, Qidi, Min Zhang, Min Xu, Weiqiong Gu, Yun Xi, Lu Qi, Biao Li, and Weiqing Wang. 2015. "Brown Adipose Tissue Activation Is Inversely Related to Central Obesity and Metabolic Parameters in Adult Human." *PloS One* 10 (4): e0123795.

Wang, Yuhui, and Hei Sook Sul. 2009. "Pref-1 Regulates Mesenchymal Cell Commitment and Differentiation through Sox9." *Cell Metabolism* 9 (3): 287–302.

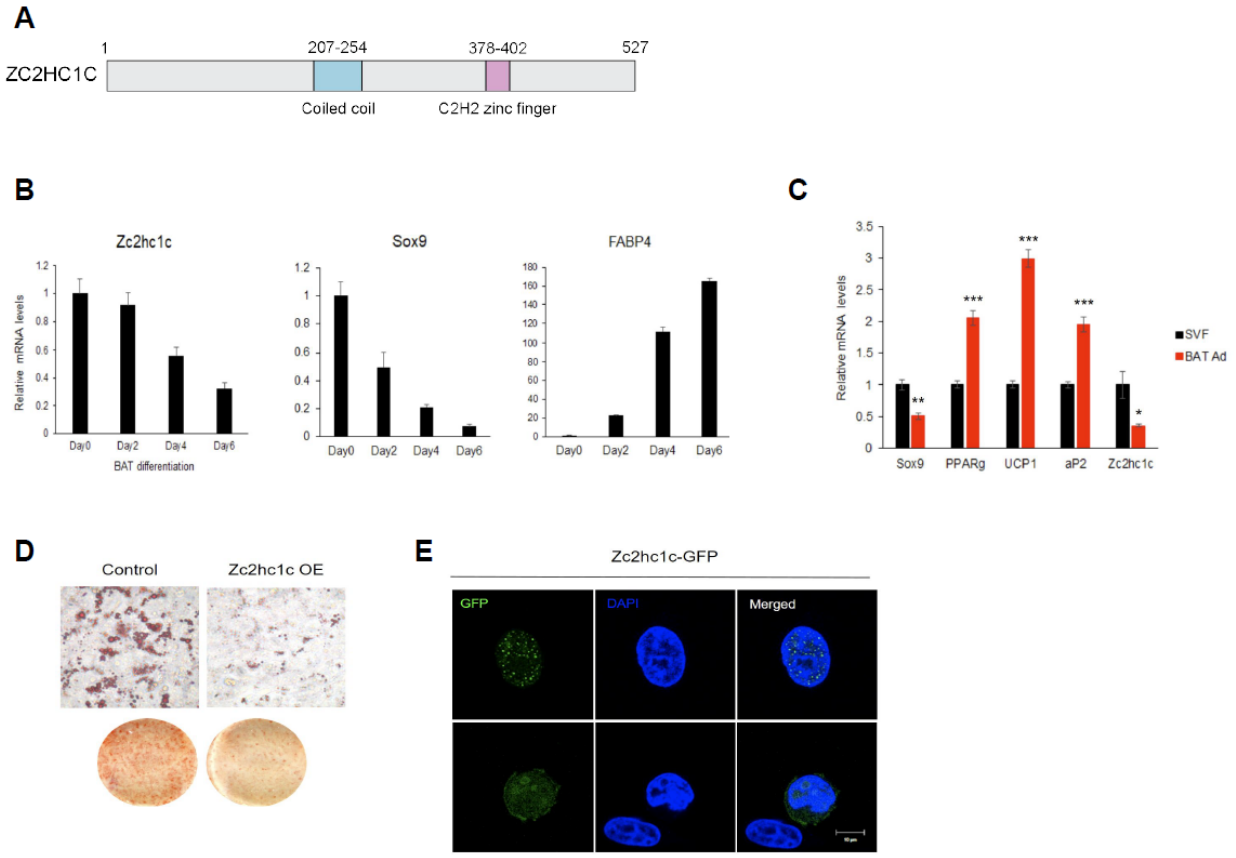


Figure 1. Characterization of Zc2hc1c.
(A) Diagram of Zc2hc1c structure. (B) qRT-PCR for the indicated genes during brown adipocyte differentiation. (C) Zc2hc1c mRNA levels in stromal vascular fraction and adipocyte fraction of BAT. (D) Oil Red O staining of control and Zc2hc1c-overexpressing cells at day 4. (E) Immunofluorescent images of Zc2hc1c-overexpressing cells.

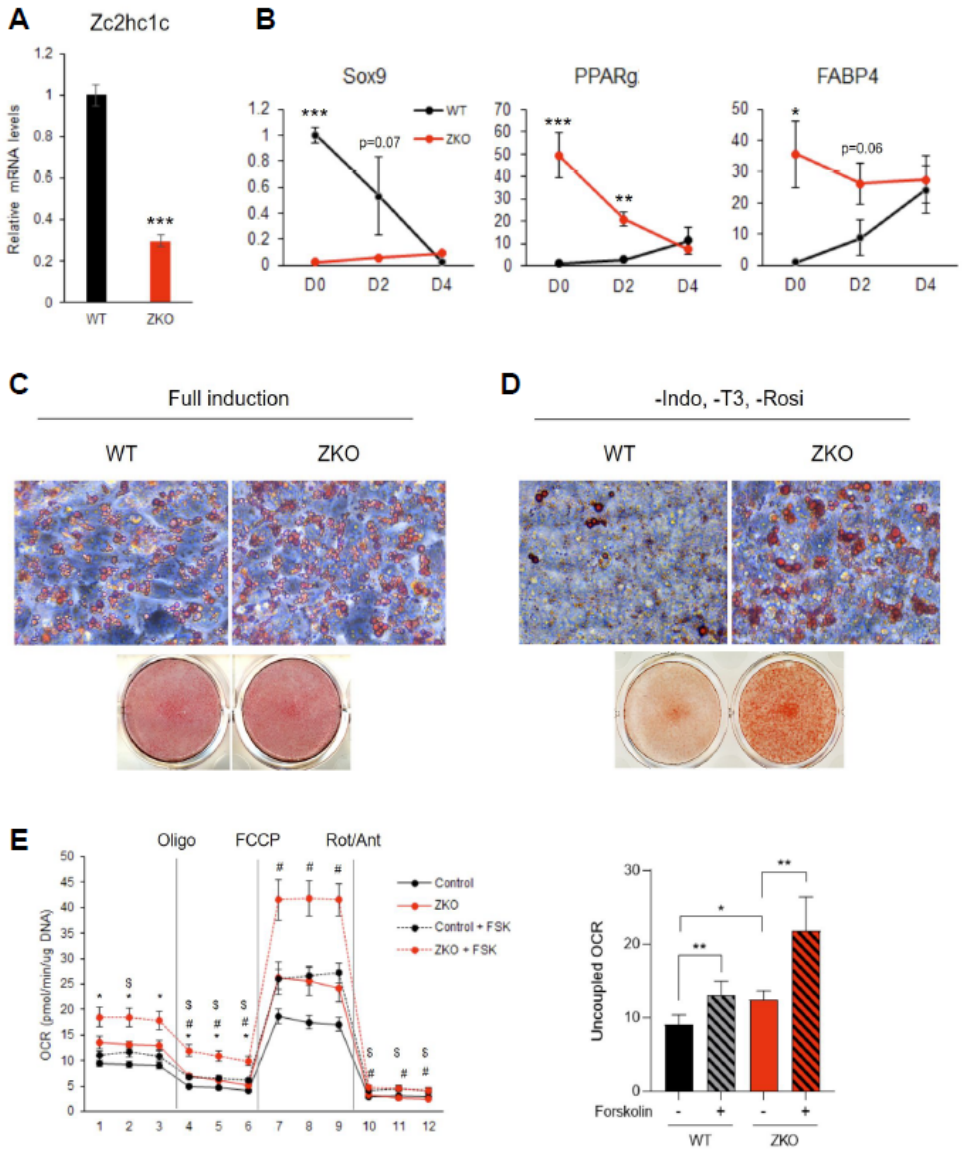
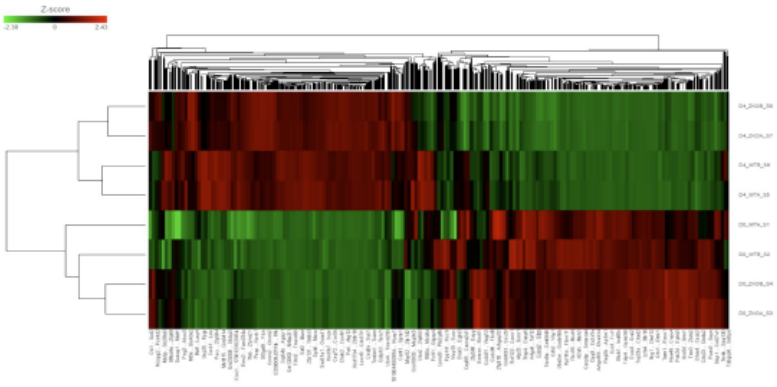
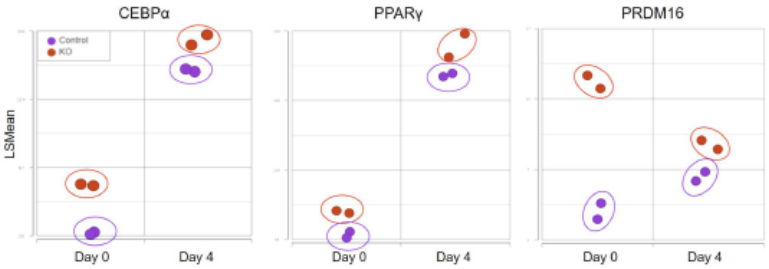


Figure 2. Zc2hc1c inhibits brown adipocyte differentiation.
(A) ZC2hC1C mRNA levels in Zc2hc1c KO cells. (B) qRT-PCR for the indicated genes during brown adipocyte differentiation. (C) Oil Red O staining at day 4 after differentiation with the regular differentiation cocktail. (D) Oil Red O staining at day 4 after differentiation without indomethacin, T3 and rosiglitazone. (E) Oxygen consumption measurement using Seahorse on day 4.

A



B



C

GO biological process	P value
metabolic process	5.07E-60
G protein-coupled receptor signaling pathway	1.44E-59
cellular metabolic process	2.66E-58
cell differentiation	4.57E-21
cellular lipid metabolic process	2.48E-07
fat cell differentiation	4.19E-06
regulation of fat cell differentiation	9.39E-06
brown fat cell differentiation	9.82E-05
glucose metabolic process	2.54E-05
regulation of fatty acid metabolic process	4.23E-04

Figure 3. RNA-sequencing of Zc2hc1c KO cells

(A) Heatmap of RNA-sequencing data. (B) mRNA levels of the indicated genes from the RNA-sequencing. (C) Gene ontology analysis of differentially expressed genes from the RNA-sequencing.

Gene	Forward	Reverse
Zc2hc1c	CAAGTGTGTGTAGGGCTTTCT	CAATCAAGGTCGCAGGGAATA
Ucp1	ACTGCCACACCTCCAGTCATT	CTTTGCCTCACTCAGGATTGG
Fabp4	ACACCGAGATTTCCTTCAAACTG	CCATCTAGGGTTATGATGCTCTTCA
Pparg	AACTCTGGGAGATTCTCCTGTTGA	TGGTAATTTCTTGTGAAGTGCTCATA
Sox9	CATCAAGACGGAGCAGCTGAG	ATGGTCAGCGTAGTCGTATTG
Eef1a1	ACGAGGCAATGTTGCTGGTGAC	GTGTGACAATCCAGAACAGGAGC

Table 1. List of primers for RT-qPCR.

Chapter 5
Conclusion

Obesity has become a worldwide epidemic, which is now prevalent not only in adults but also in children (Caballero 2007; Han, Lawlor, and Kimm 2010). Since it is caused by excess energy intake, researchers have been looking for ways to increase energy expenditure to restore the balance between energy intake and expenditure (Romieu et al. 2017). One way to increase energy expenditure is through thermogenesis in brown adipocytes (Yoneshiro et al. 2011). In addition, inguinal white adipose tissue (iWAT) undergoes a process called browning/beiging, where some cells in iWAT depots become beige adipocytes to gain thermogenic ability (Bartelt and Heeren 2014). Brown and beige adipocytes express the key protein for thermogenesis, uncoupling protein 1 (UCP1), which leaks protons in the mitochondrial intermembrane space into the mitochondrial matrix, resulting in heat production (Nedergaard and Cannon 2018). UCP1 activity and expression are stimulated by β_3-adrenergic signaling, which is activated by certain stimuli such as cold exposure. There are other pathways known to affect adipose thermogenesis, such as insulin/IGF1 signaling, thyroid hormone and TGFβ signaling (Tabuchi and Sul 2021). Insulin/IGF1 signaling promotes thermogenesis mainly through enhancing BAT development and browning of iWAT. Thyroid hormone binds thyroid hormone receptors to upregulate the transcription of thermogenic genes including UCP1. In contrast, TGFβ signaling suppresses adipose thermogenesis. Furthermore, recent studies reported the existence of UCP1-independent thermogenic mechanisms such as calcium cycling and creatine-phosphocreatine cycling (Ikeda et al. 2017; Kazak et al. 2015). Thus, we sought to discover novel thermogenic factors in adipocytes, regardless of whether they are UCP1-dependent or not.

To do so, we performed multiple genome-wide CRISPR-Cas9 screening in brown adipocytes. From the screening using a temperature-sensitive dye, ERthermAC, we found Apold1 as a new thermogenic factor, whose function is completely unknown in adipocytes. Apold1 is cold inducible and highly expressed in BAT with numerous GWAS data associated with metabolism. *In vitro* experiments of Apold1 confirmed that Apold1 indeed promotes thermogenesis. Moreover, overexpression of Apold1 via virus injection into BAT increased body temperature after cold challenge and oxygen consumption in mice. It would also be important to generate and examine BAT-specific Apold1 knockout and overexpression in mice. Based on the increase and decrease in uncoupled oxygen consumption upon overexpression and knockout of Apold1, respectively, we propose that Apold1 is involved in UCP1-dependent thermogenesis. Given that Apold1 localizes at the plasma membrane, next steps would be to look at early components of β_3-adrenergic signaling such as cAMP levels and PKA activity. Unbiased approaches such as identification of interacting partners through co-immunoprecipitation followed by mass spectrometry should also be taken to dissect how Apold1 works to promote thermogenesis.

Another screening we conducted used JC-1 dye as a readout, which senses mitochondrial depolarization and thus serves as an indicator for thermogenesis. We found Rasl12, which was enriched in BAT at both mRNA and protein levels compared to other tissues examined. While Rasl12 knockout in brown adipocytes caused a decrease in thermogenesis, Rasl12

overexpression increased thermogenesis measured by ERthermAC and Seahorse Assay. Animal studies should be conducted to investigate its physiological role *in vivo*. Interestingly, Rasl12 localizes at nuclear envelope. Co-immunoprecipitation experiments identified nuclear transport machinery and numerous mRNA processing factors as its potential interacting partners. We were able to confirm the interaction of Rasl12 with Xpo1 and Kpnb1. Although there has been no studies that examined the nuclear transporters in the context of adipose tissue thermogenesis, it has been reported that alternative splicing of thermogenic genes such as Pparγ and Prdm16 are important for adipocyte function. Thus, Rasl12 might promote thermogenesis via nuclear transport and/or mRNA processing of thermogenic genes.

Lastly, another screening was performed to identify new differentiation factors for brown adipocytes. Zc2hc1c was identified as a potential candidate to follow up since Zc2hc1c expression was enriched in stromal vascular fraction and was decreased over the course of differentiation. Overexpression of Zc2hc1c indeed inhibited brown adipocyte differentiation. However, in this experiment GFP-tagged Zc2hc1c for immunofluorescent detection for its overexpression was used and non-tagged Zc2hc1c should also be used for confirmation. Regardless, Zc2hc1c knockdown resulted in enhanced brown adipocyte differentiation, as judged by the Oil Red O staining and RNA-sequencing data. The DNA binding site/sequence of Zc2hc1c, potential interacting partners as well as the role of Zc2hc1c in mouse models will further demonstrate its role and underlying mechanism in brown adipocyte differentiation.

All together, these studies provide novel insights into the mechanisms of thermogenesis and differentiation in brown adipocytes. Although the above genes were initially identified in brown adipocytes, their roles should also be investigated in beiging of brown adipocytes, which is suggested to be the dominant thermogenic adipocytes in human adults.

References

Bartelt, Alexander, and Joerg Heeren. 2014. "Adipose Tissue Browning and Metabolic Health." *Nature Reviews. Endocrinology* 10 (1): 24–36.

Caballero, Benjamin. 2007. "The Global Epidemic of Obesity: An Overview." *Epidemiologic Reviews* 29 (June): 1–5.

Han, Joan C., Debbie A. Lawlor, and Sue Y. S. Kimm. 2010. "Childhood Obesity." *The Lancet* 375 (9727): 1737–48.

Ikeda, Kenji, Qianqian Kang, Takeshi Yoneshiro, Joao Paulo Camporez, Hiroko Maki, Mayu Homma, Kosaku Shinoda, et al. 2017. "UCP1-Independent Signaling Involving SERCA2b-Mediated Calcium Cycling Regulates Beige Fat Thermogenesis and Systemic Glucose Homeostasis." *Nature Medicine* 23 (12): 1454–65.

Kazak, Lawrence, Edward T. Chouchani, Mark P. Jedrychowski, Brian K. Erickson, Kosaku Shinoda, Paul Cohen, Ramalingam Vetrivelan, et al. 2015. "A Creatine-Driven Substrate Cycle Enhances Energy Expenditure and Thermogenesis in Beige Fat." *Cell* 163 (3): 643–55.

Nedergaard, Jan, and Barbara Cannon. 2018. "Brown Adipose Tissue as a Heat-Producing Thermoeffector." *Handbook of Clinical Neurology* 156: 137–52.

Romieu, Isabelle, Laure Dossus, Simón Barquera, Hervé M. Blottière, Paul W. Franks, Marc

Gunter, Nahla Hwalla, et al. 2017. “Energy Balance and Obesity: What Are the Main Drivers?” *Cancer Causes & Control: CCC* 28 (3): 247–58.
Tabuchi, Chihiro, and Hei Sook Sul. 2021. “Signaling Pathways Regulating Thermogenesis.” *Frontiers in Endocrinology* 12 (March): 595020.